EUROfusion

ENR-MAT.01.UT 2021-2024 Report

Investigation of defects and disorder in nonirradiated and irradiated Doped Diamond and Related Materials for fusion diagnostic applications (DDRM) – Theoretical and Experimental analysis

Aleksandr Lushchik

University of Tartu ESTONIA — *UT*

LATVIA — *ISSP-UL*

Karlsruhe Institute of Technology GERMANY — *KIT*

Consortium:

Institute of Physics, University of Tartu – *UT*, A. Lushchik)
Karlsruhe Institute of Technology, Germany – *KIT*, T. Scherer
Institute of Solid State Physics, Latvian University – *ISSP-UL*, A. Popov

This work has been carried out within the framework of the EUROfusion Consortium, funded by the European Union via the Euratom Research and Training Programme (Grant Agreement No 101052200 — EUROfusion). Views and opinions expressed are however those of the author(s) only and do not necessarily reflect those of the European Union or the European Commission. Neither the European Union nor the European Commission can be held responsible for them.

Our **goal** is to combine experimental investigations of new functional materials used in diagnostics, heating and current drive applications in fusion reactors with large-scale theoretical calculations to provide an exhaustive understanding of material behaviour and predict the corresponding properties which are of high relevance for DEMO.

Combination of traditional techniques (optical absorption, IR spectroscopy, luminescence, EPR) with Raman and neutron scattering, determination of electrical/microwave properties via high frequency FABRY-PEROT-resonators and THz spectroscopy and electrical and thermal conductivity measurements in order to **monitor the development of the radiation damage** in doped diamond and related materials. Of great importance – determination of a specific role of impurities, which could improve/worsen radiation resistance.

The main project tasks are divided between four Work Packages:

WP1. Advanced characterization of functional materials before and after irradiation

WP2. Investigation of electric, dielectric and mechanical properties of nonirradiated and irradiated materials

WP3. Theoretical modelling of the doping and radiation-induced effects

WP4. Material expertise for fusion applications (series of meetings)

*Mainly CVD diamond disks – polycrystalline samples of different diameter produced via **C**hemical **V**apor **D**eposition by Diamond Materials, Freiburg (Germany), only a few single crystal diamond (SCD) samples*

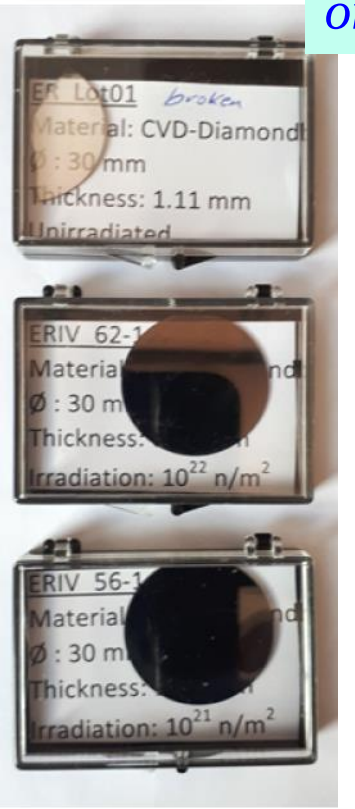

d =30 mm

neutron-irradiated/pristine samples

Sample No.	***Material***	***Diameter***	***Thickness***	***Irradation***
		mm	mm	n/m^2
ERIV_62-1	CVD-Diamond	30	0,69	1E+22
ERIV_56-1	CVD-Diamond	30	1,31	1E+21
ER_Lot10	CVD-Diamond	30	1,11	1E+24
ER_Lot01	CVD-Diamond	30	1,11	0
3Qu04	Silica	30	1,005	1E+22
4Qu04	Silica	30	3,041	1E+22
3Qu07	Silica	30	1	1E+21
4Qu07	Silica	30	3	1E+21
4Qu09	Silica	30	3	0
Al_146	Alumina	40	4	0
Al_166	Alumina	40	4	0

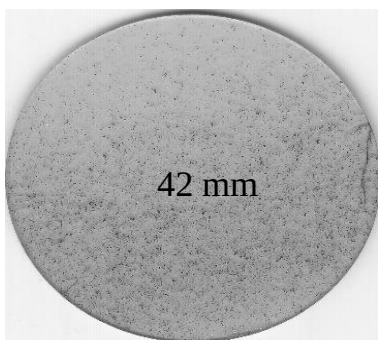

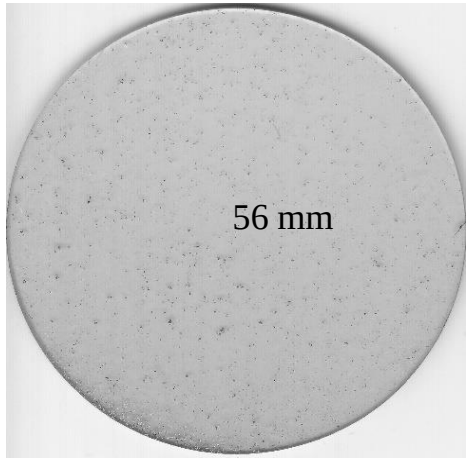

Irradiation by 36-MeV ^{127}I ions, 5-mm disks

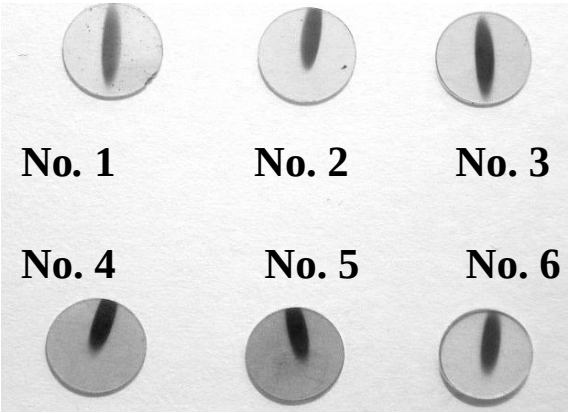

Irradiation by 231-MeV ^{132}Xe ions

d = 5 mm

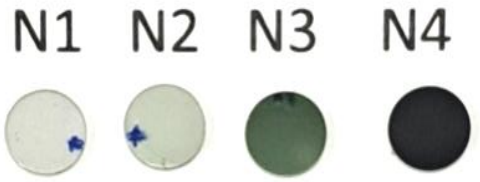

10^{11} 10^{12} 10^{13} 3.8×10^{13} Xe/cm^2

University of Tartu
ESTONIA

Characterization of virgin/irradiated materials via cathodoluminescence (steady-state regime, 10-keV electron beam, 5 or 295 K

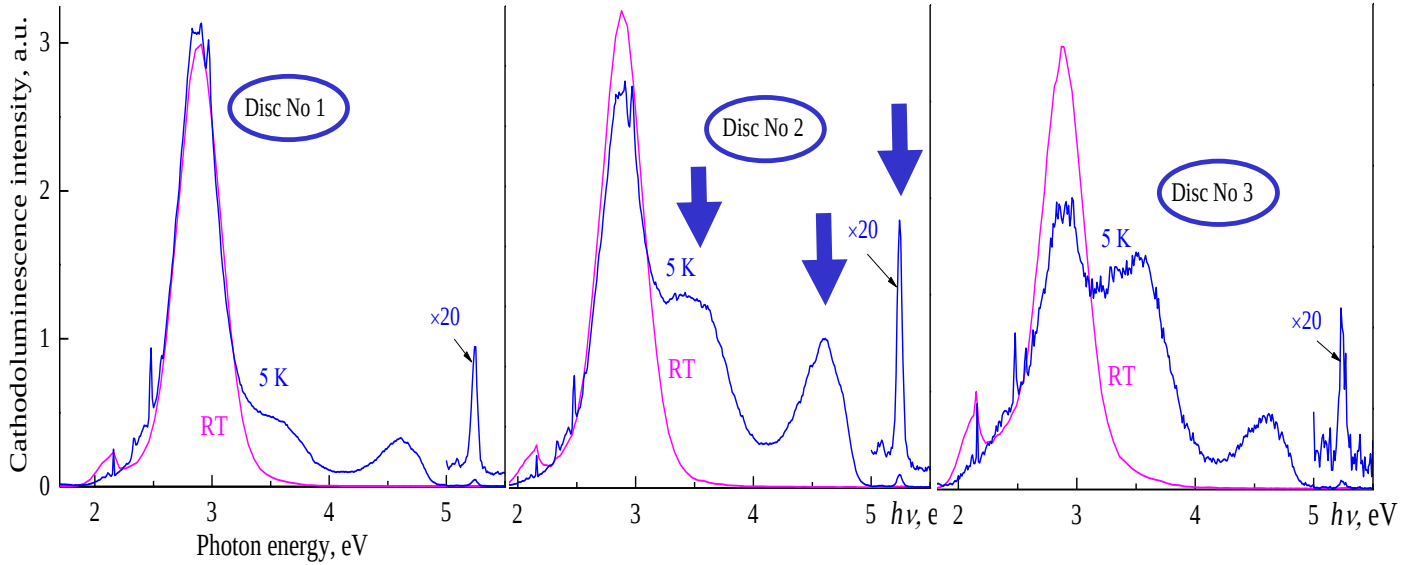

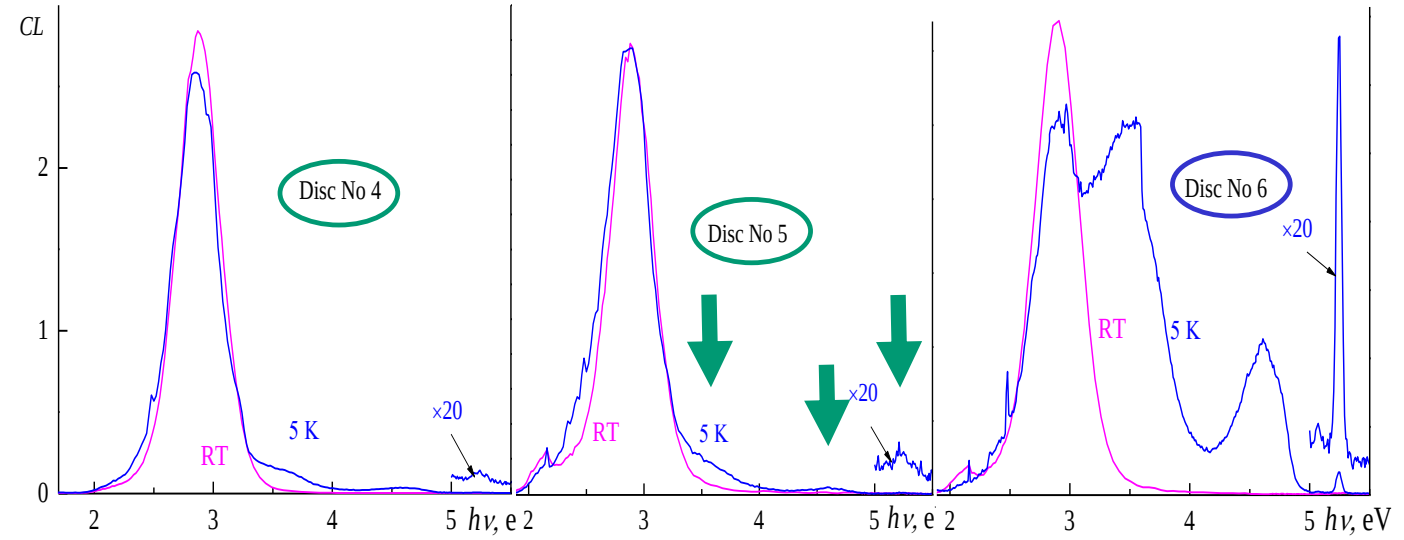

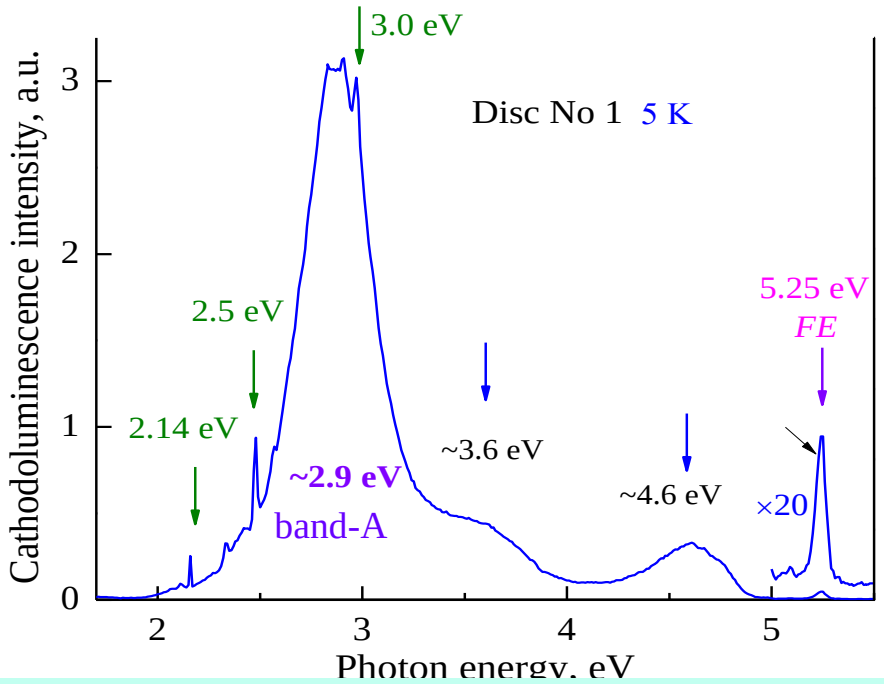

The #1 set of pristine 5-mm CVD diamond disks. CL spectrum varies from sample to sample

Drastic (about **two orders of magnitude**) and **spectrally not selective** drop of CL intensity in *Iodine*-irradiated samples.

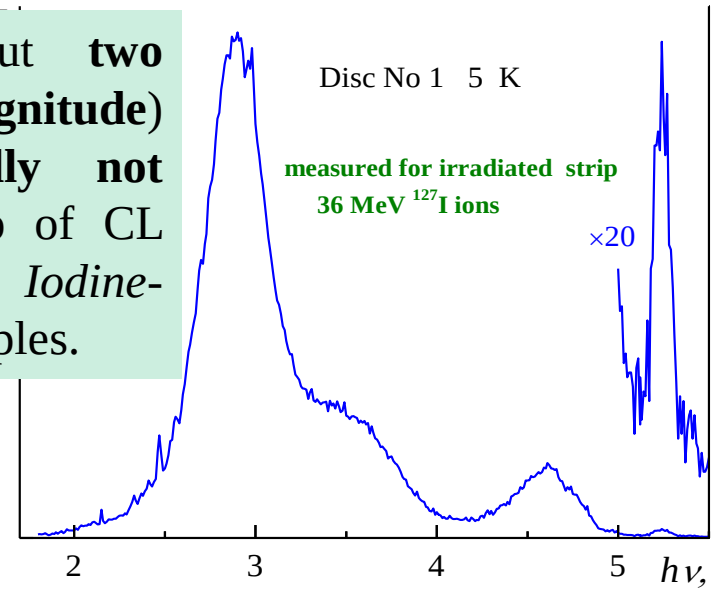

University of Tartu
ESTONIA

Characterization of virgin/irradiated materials via cathodoluminescence (steady-state regime, 10-keV electron beam, 5 or 295 K

The #2 set of pristine5-mm CVD diamond disks, before and after irradiation with 231-MeV Xe ions

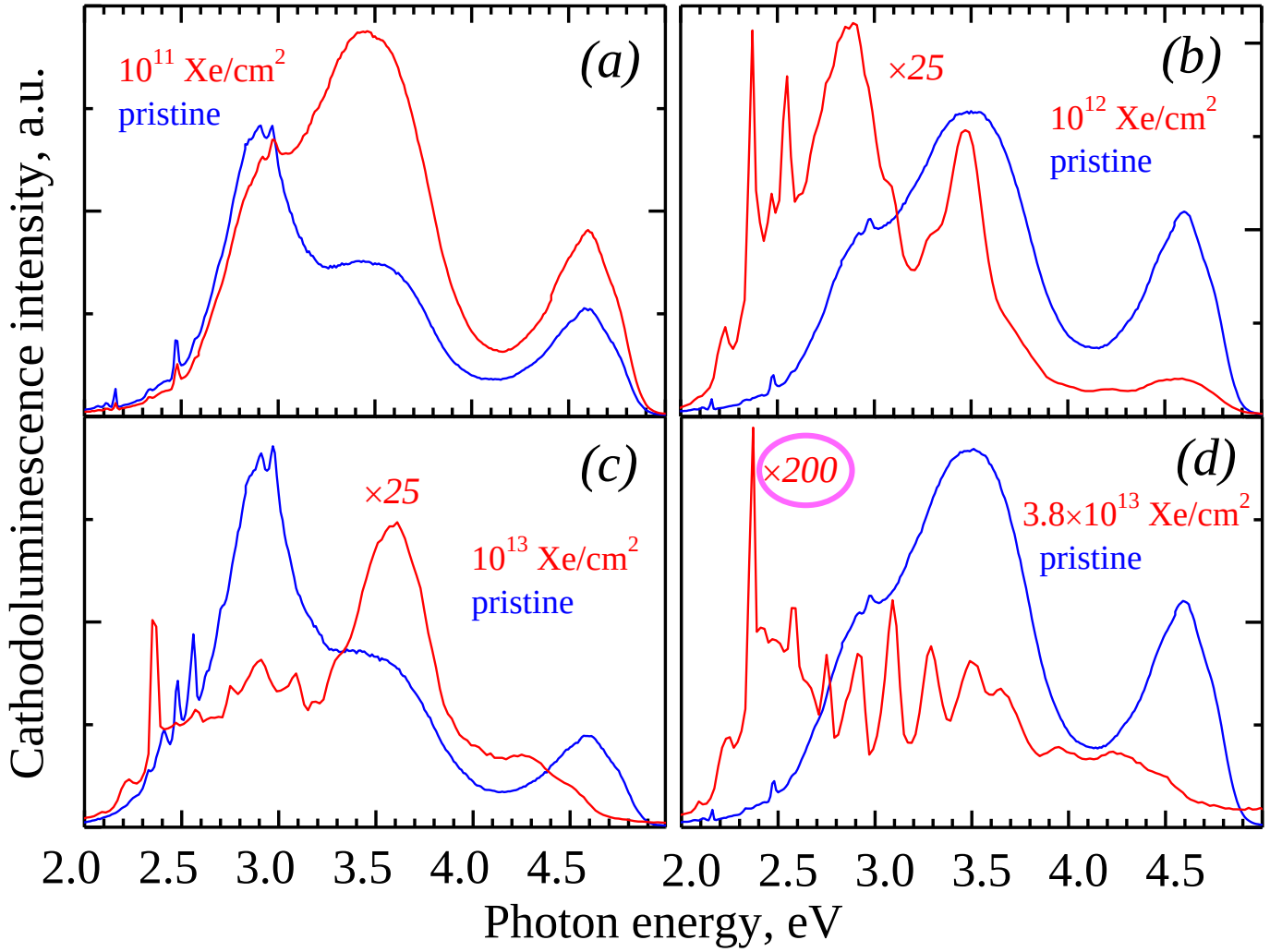

Again, new pristine samples do not demonstrated the heterogeneity estimated via CL. As a result, the analysis of CL spectra for Xe-irradiated discs did not allow to establish a clear fluence-effect relationship.

Figure. Steady-state CL spectra measured at 5 K under 10-keV electron excitation of CVD diamond disks before (pristine, blue lines) and after expose to 231-MeV xenon ions with different fluences (red lines). Ordinates of some curves for irradiated samples are multiplied by a prescribed factor.

2D mapping of virgin & neutron-irradiated CVD samples by cathodoluminescence spectra

∅ up to 30 mm

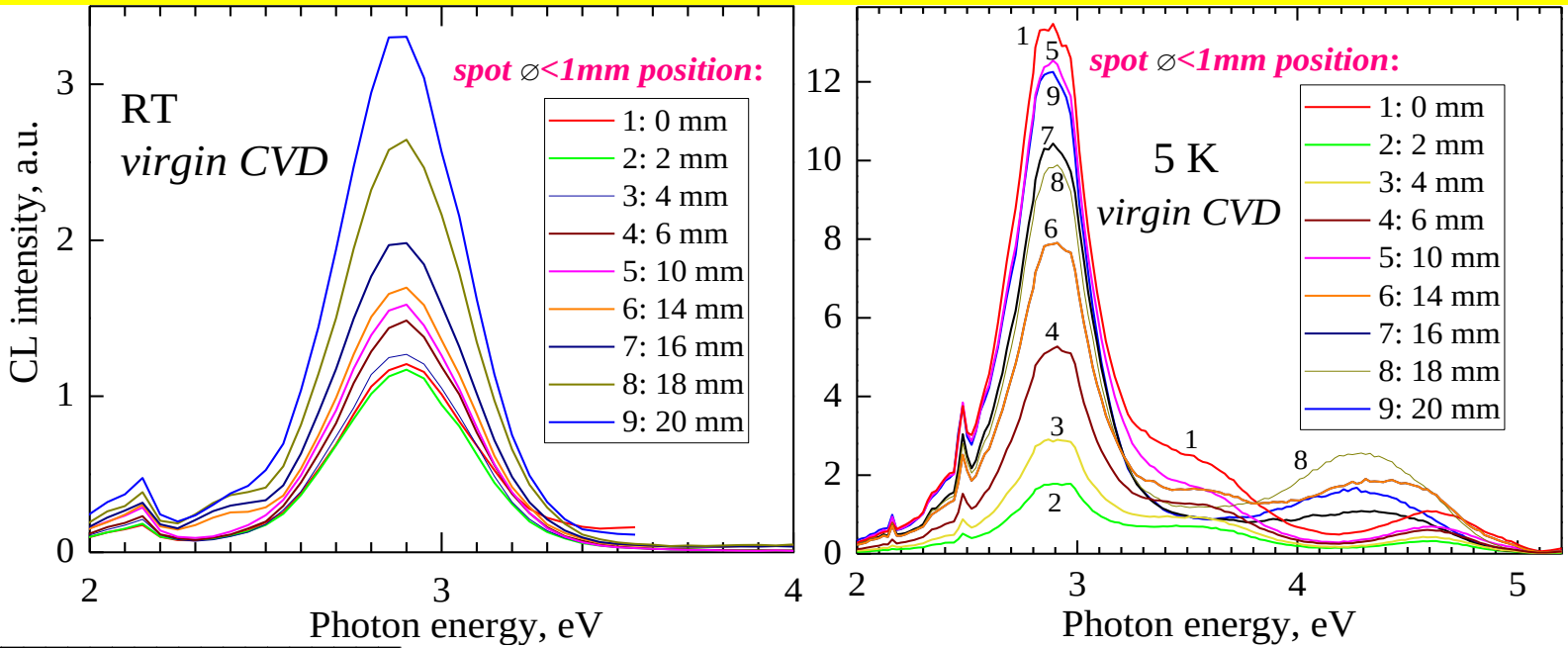

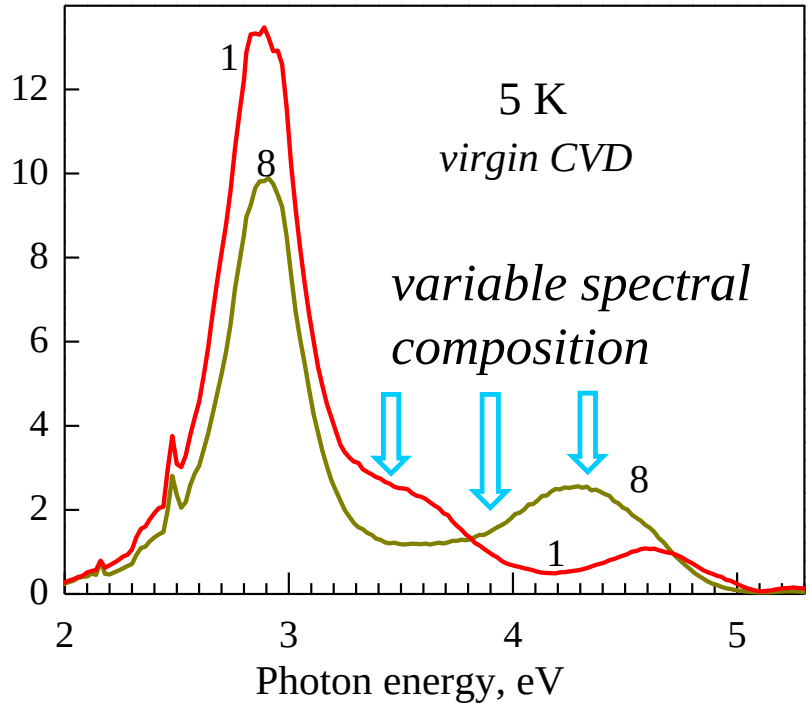

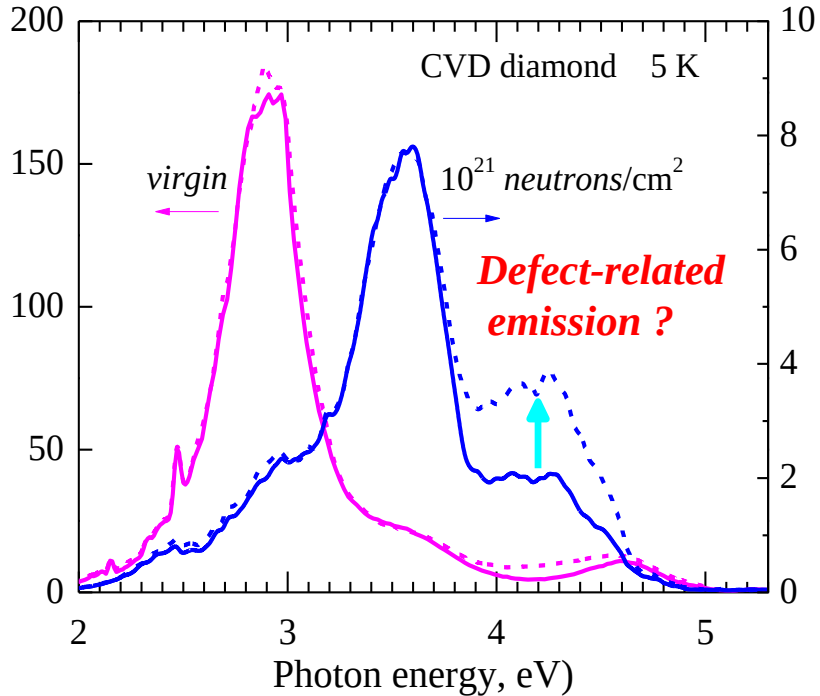

CL spectra for a virgin and *n*-irradiated samples at the beginning (solid lines) and after 15-min excitation by an e-beam (dashed lines).

Characterization of virgin/neutron irradiated CVD diamond via infrared spectroscopy (ISSP-UL)

INSTITUTE OF SOLID STATE PHYSICS
UNIVERSITY OF LATVIA

LATVIA

Spectrometer Vertex 80v (Bruker)
Resolution = 2 cm^{-1}

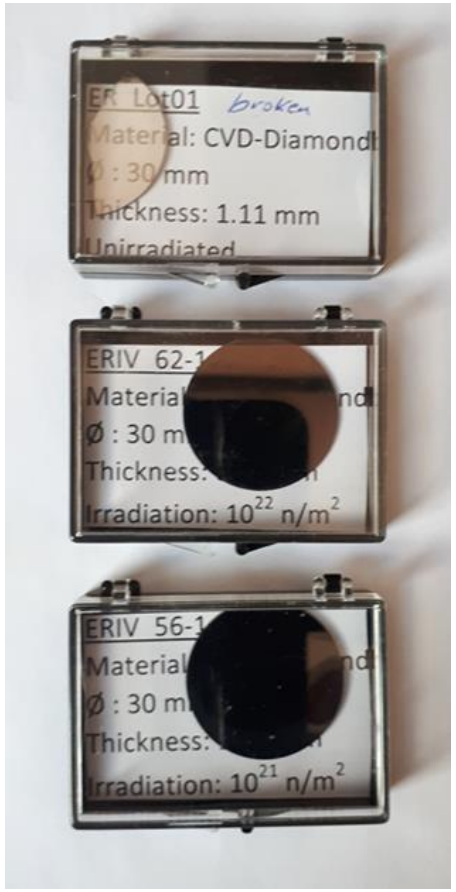

rich radiation-induced vibrational structure

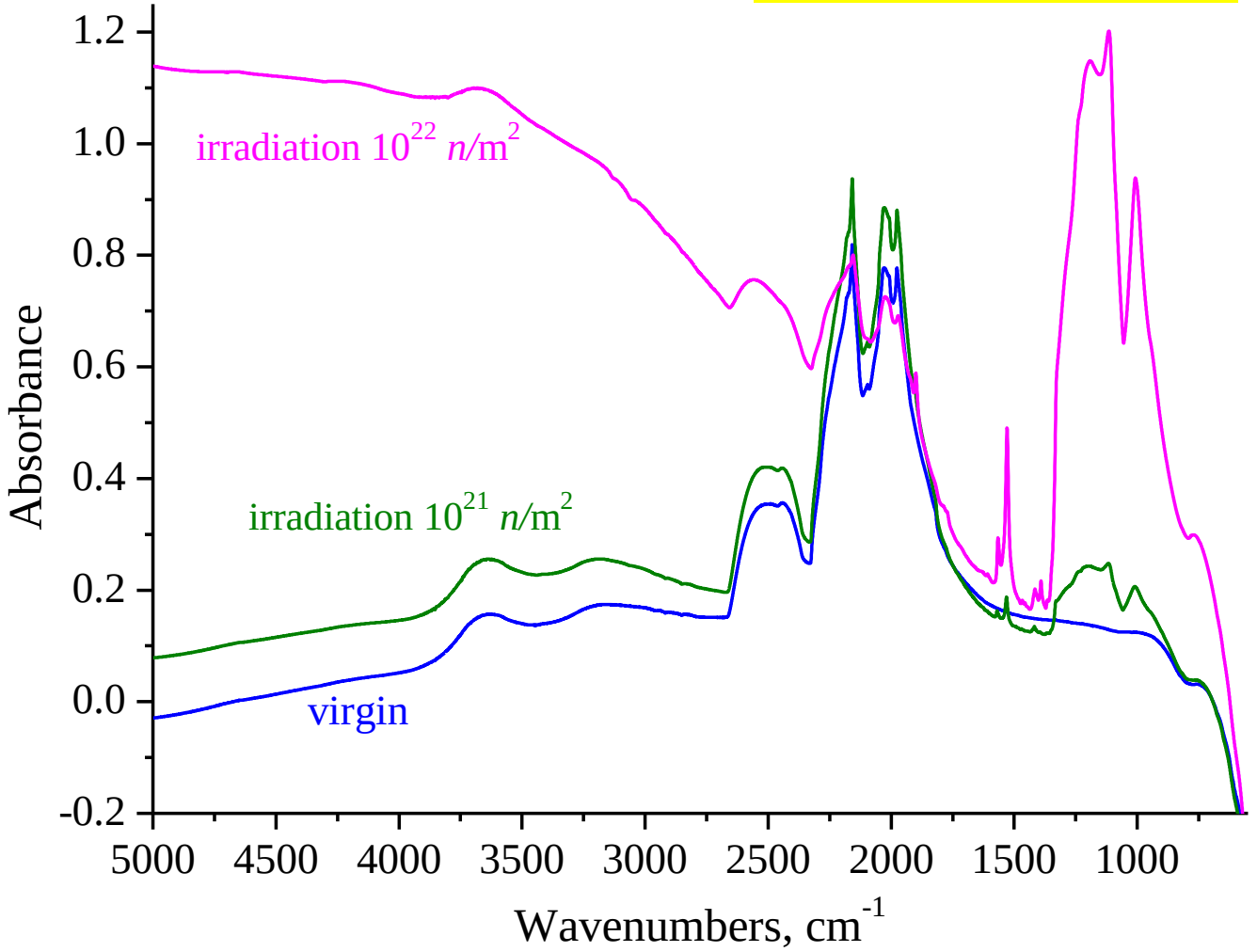

5000 cm^{-1} = 0.62 eV
1000 0.124
10000 1.24 eV

INSTITUTE OF SOLID STATE PHYSICS
UNIVERSITY OF LATVIA
LATVIA

Characterization of CVD diamond via Raman (UT, ISSP-UL)

2D Mapping of large diamond disks

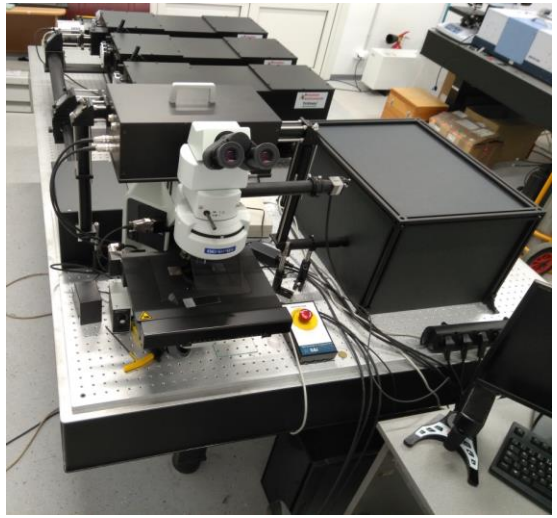

TriVista Raman spectrometer

Raman shift, cm^{-1}	Literature interpretation
1400	Nitrogen center NV^0
3100	Nitrogen center NV^-
5200	Silicon center SiV

Luminescence and **microscope** image

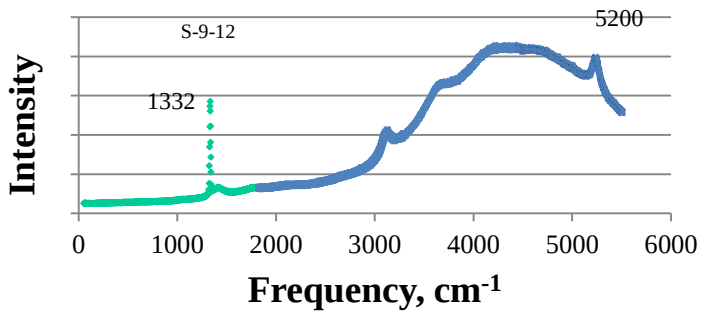

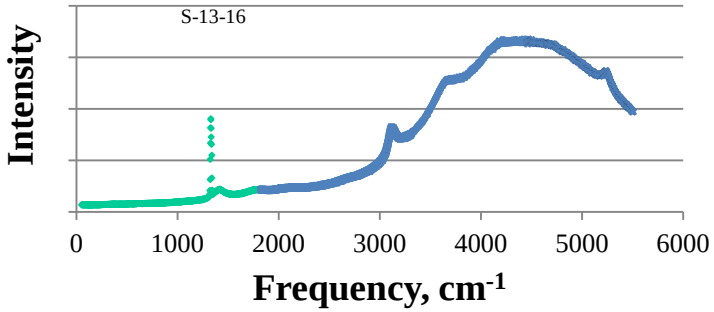

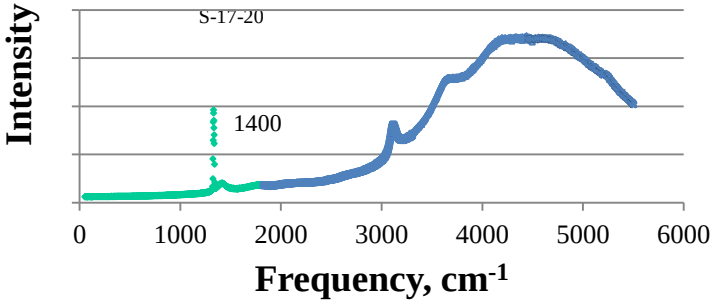

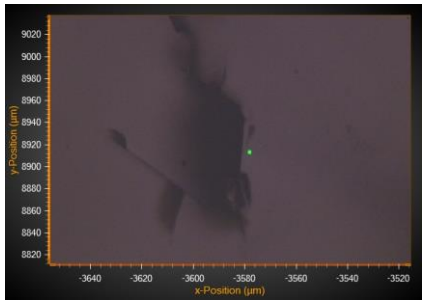

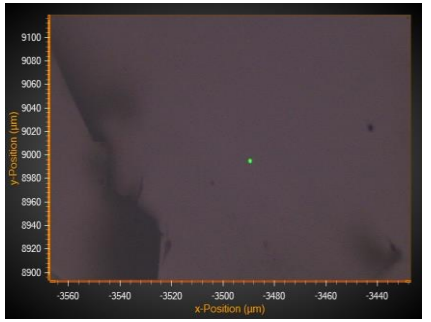

Luminescence spot position (532-nm laser excit.)

a *on a dark inclusion*

b *close to a dark inclusion*

c *far from a dark inclusion*

Comparative analysis/ 2D mapping of pristine/231-MeV Xe-irradiated CVD disks (ISSP-UL)

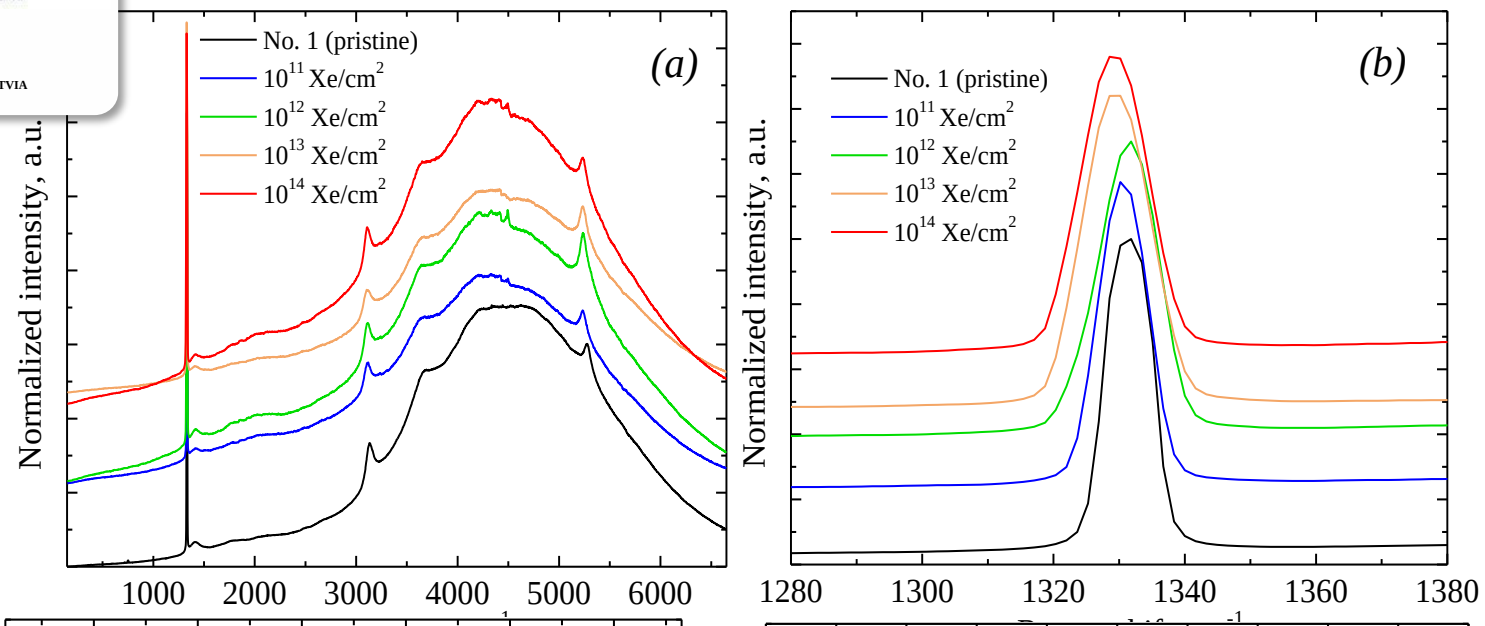

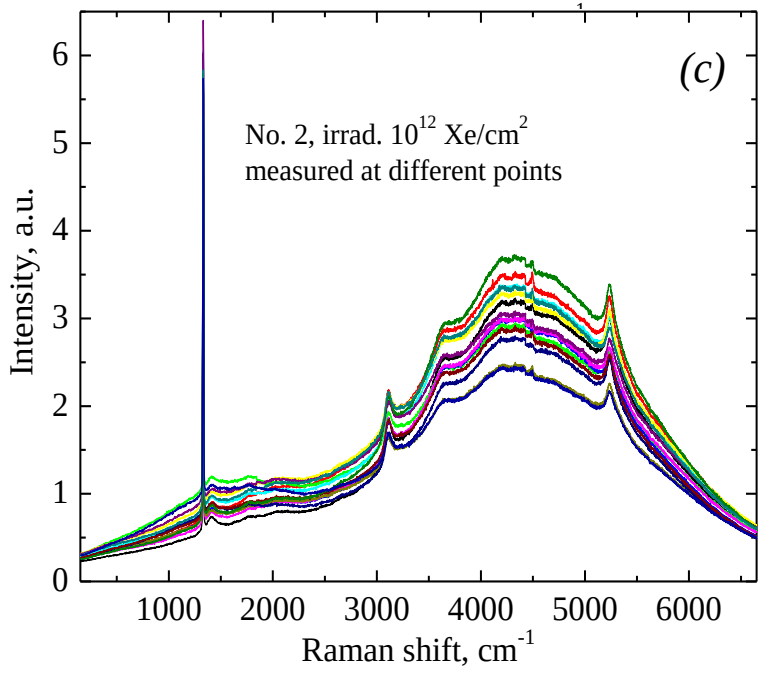

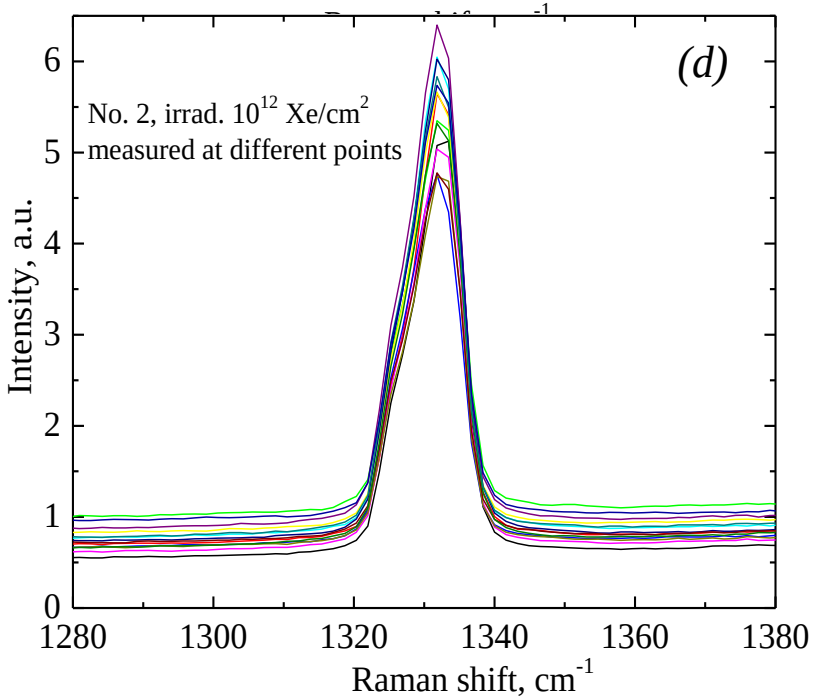

… via Raman spectroscopy

Raman spectra contain a single mode at 1332 cm^{-1}. The bands related to nitrogen vacancies (NV^0 at 1400 and NV^- at at 3100 cm^{-1}) – ***no substantial changes*** for pristine and irradiated CVD disks.

The 1332-cm^{-1} modes (see part *b*) broadens, shifts to lower frequencies, and transforms to asymmetric with irradiation fluence – ***a local structural disorder*** induced in diamond samples by Xe-irradiation.

Parts *(c)* and *(d)* – 2D mapping

Figure. Raman spectra of CVD diamond disks before and after expose to 231-MeV Xe ions with different fluence. The spectra are measured at 14 different spot positions of 525-nm laser excitation on disk No. 2 irradiated with 10^{12} Xe/cm^2 (*2D*-mapping – parts *(c)* and *(d)* for different spectral regions).

Comparative analysis/ 2D mapping of pristine/231-MeV Xe-irradiated CVD disks (ISSP-UL)

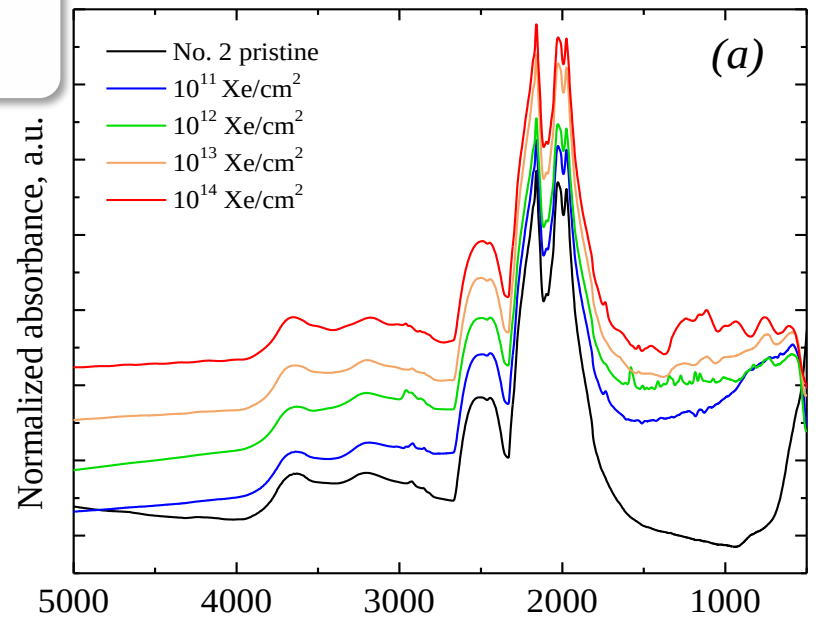

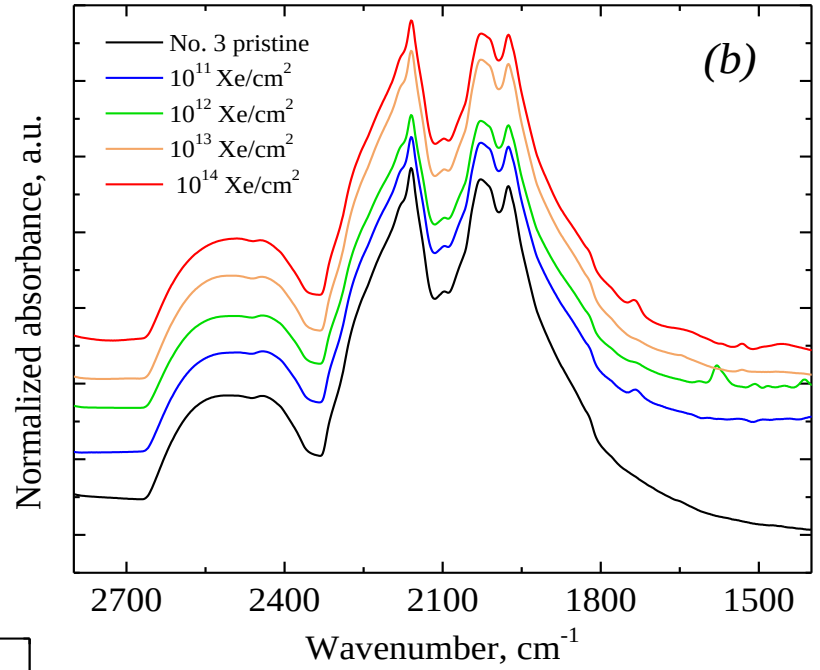

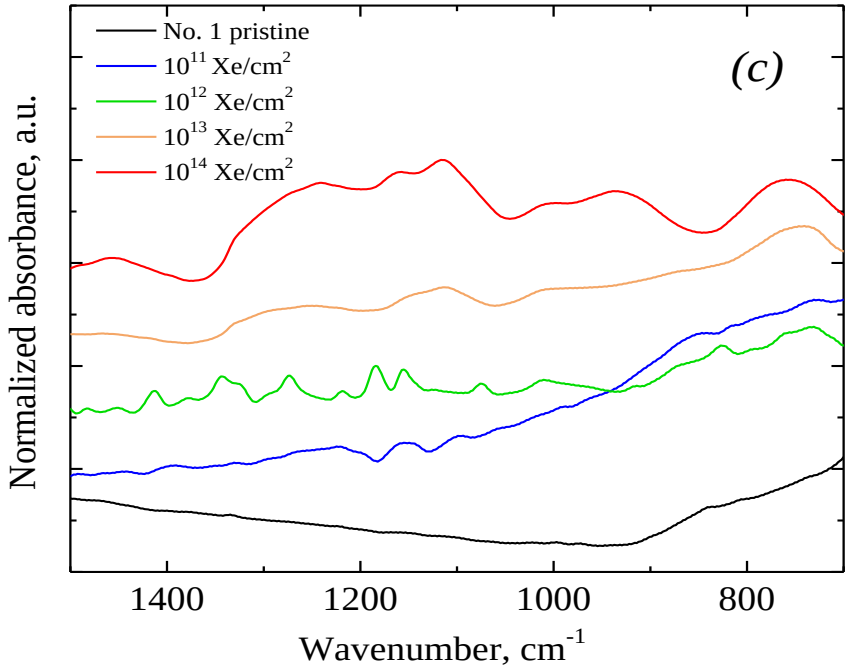

Figure. FTIR absorbance spectra of CVD diamond disks before (pristine) and after expose to 231-MeV xenon ions with different fluence. The spectra are similar for all four disks under investigation (labelled by number in a relevant figure part).

… via FTIR

b - the characteristic C–C band at 2600-1600 cm^{-1} shows **no significant alteration** before and after Xe-irradiation of diamond.

c - Irradiation → <u>appearance of nitrogen defect</u> bands 1700-500 cm^{-1}. This change likely relates to a modification in the state of N defects.

Electron backscatter diffraction in boron-doped CVD diamond)

Karlsruhe Institute of Technology
GERMANY

The *p*-doping level of Boron atoms was estimated using Van der Pauw method as

~ 2×10^{18} cm^{-3}

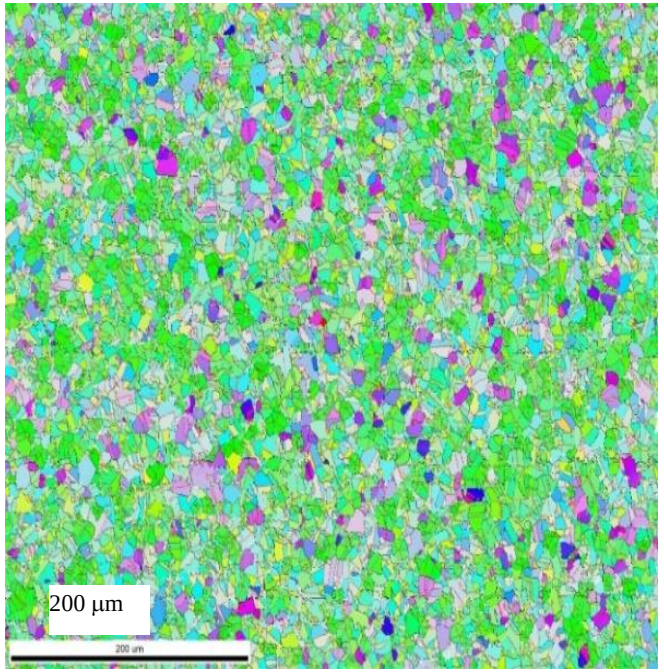

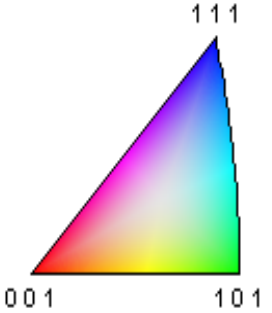

EBSD chart for a *p*-Boron-doped CVD diamond (with the directions parallel to the growth direction. Color coded map: Inverse pole [001] crystal direction (growth direction). Miller Index legend to the color scheme.

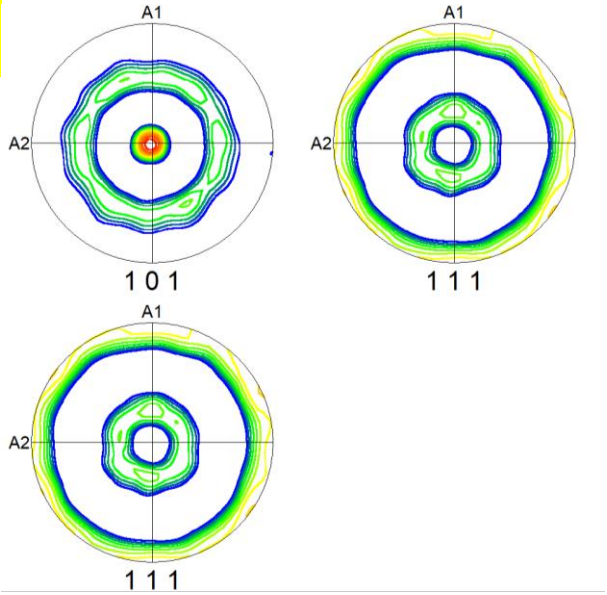

Pole pictures for the [101], [111] and [111] directions (*upper* part) and a misorientation chart (*lower* part) for a B-doped diamond.

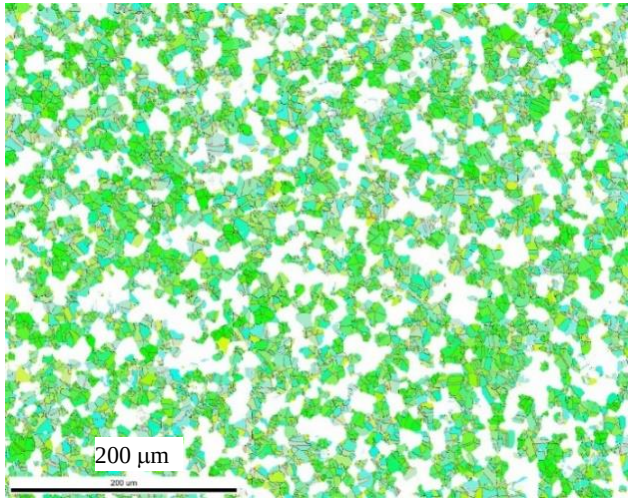

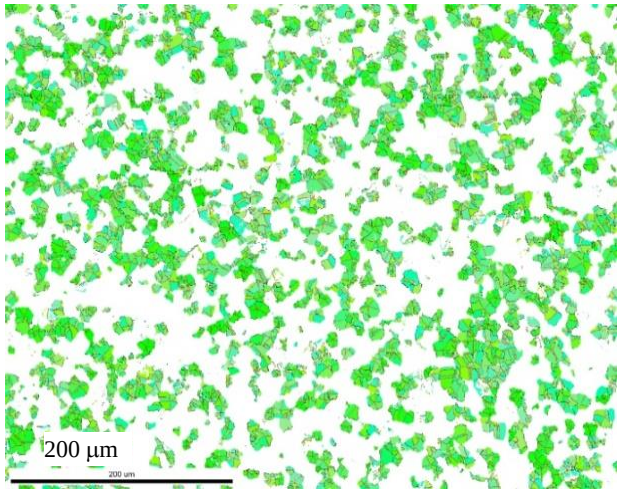

EBSD charts for a B-doped CVD diamond with all grains in a 15° tolerance field related to the [110] direction (*left* part, 65% of area) and the same for 10° (*right*, 40% of area).

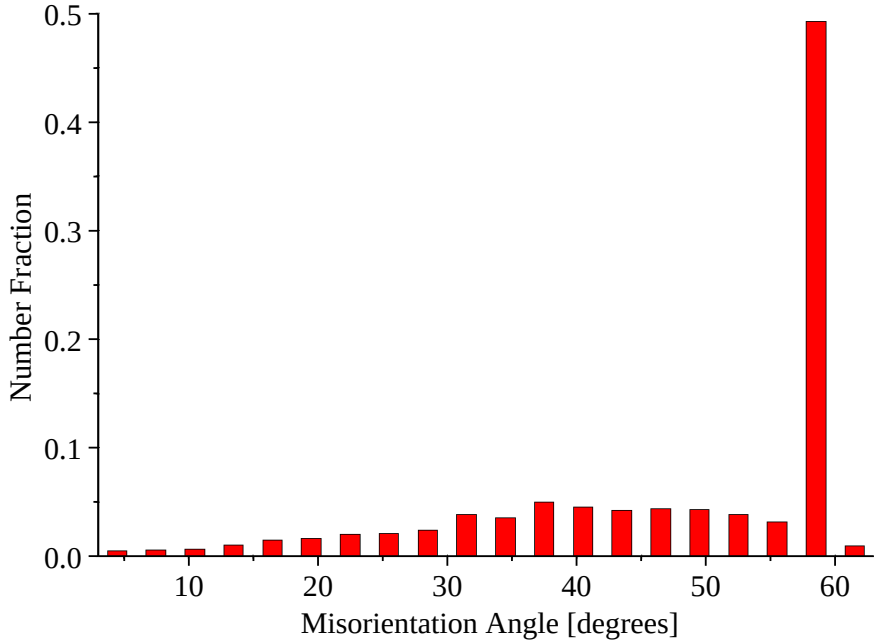

Karlsruhe Institute of Technology
GERMANY

The crystallographic properties of a **single crystalline diamond** **passivated** with a layer of SiO (ca. 100 nm thick)

The uncoated side (*left*) is a perfect single crystal without any grain boundaries.
According to the EBSD data, the SiO-coating is presumably not crystalline (no diffraction patterns in undamaged coated areas).
Green-colored regions – a small damage of the SiO surface due to sample handling (*right*).

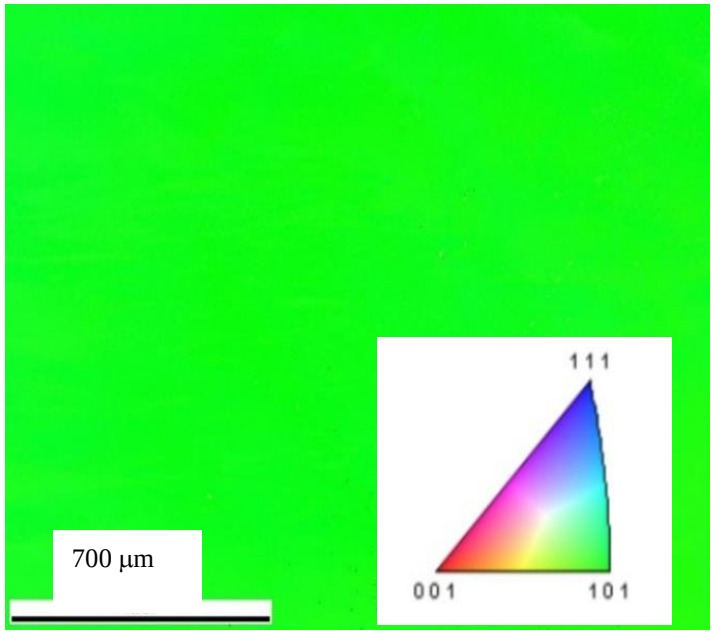

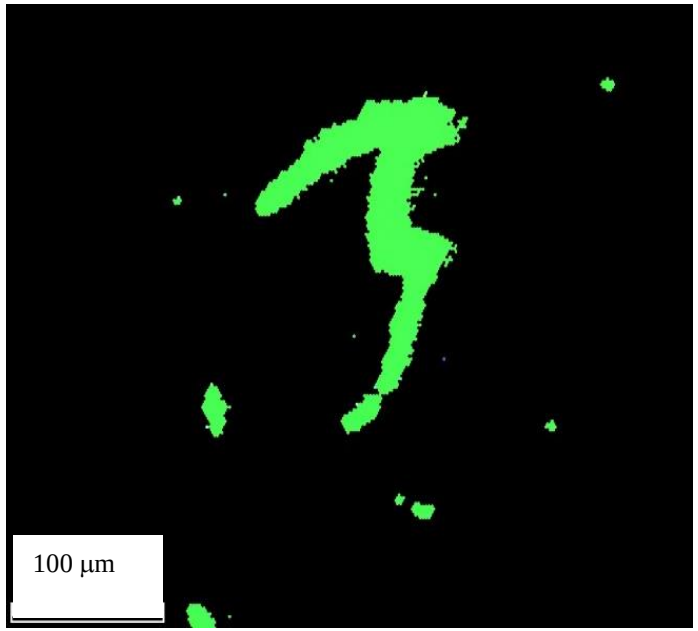

SiO – Sublimation evaporation

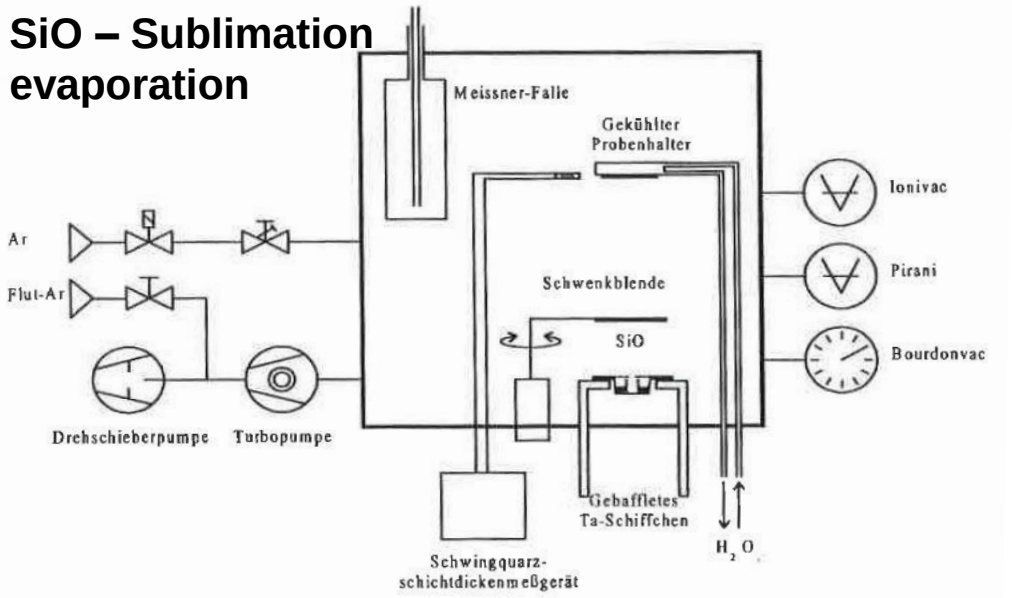

EBSD charts for a single crystal diamond (left, inverse poole mapping) and SiO-coated side with a green-colored damaged regions (right). Pole figures for the basic crystallographic directions for the uncoated side.

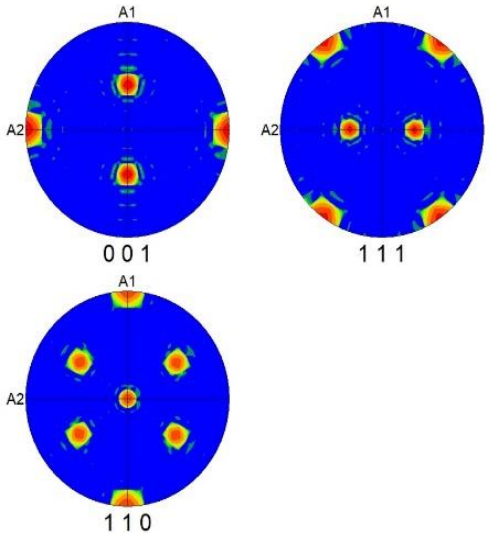

Plans (Task specification) for 2023

Report 31/12/2023

1. Literature review on radiation defect thermal annealing in selected materials — ***Fully***
2. Comparative analysis of the thermal annealing of radiation damage via OA, EPR, TSL, RAMAN/IR of the selected samples irradiated at different fluences — ***Fully***
3. Computational modelling of the influence of radiation-induced disordering on the annealing kinetics of radiation defects in diamond — ***Fully***
4. Detailed comparative analysis of dielectrical electrical, and EBCSD properties of selected materials irradiated with varying fluences ***DONE*** — ***Partly***
5. EBSD measurements of both diamond types and the interface passivation layers — ***Fully***
6. First principles calculations of radiation defects in AlN and SiO
7. Comparative 2D mapping of the oversized irradiated samples by Raman, IR and CL — ***Fully***
8. Modeling of radiation defect annealing in AlN and SiO.
9. Comparative inelastic and small angle neutron scattering of selected heavily irradiated samples at ILL ***TRIED*** — ***Partly***

Karlsruhe Institute of Technology
GERMANY

Electron backscatter diffraction (***EBSD***) – grain orientation in polycrystalline diamond

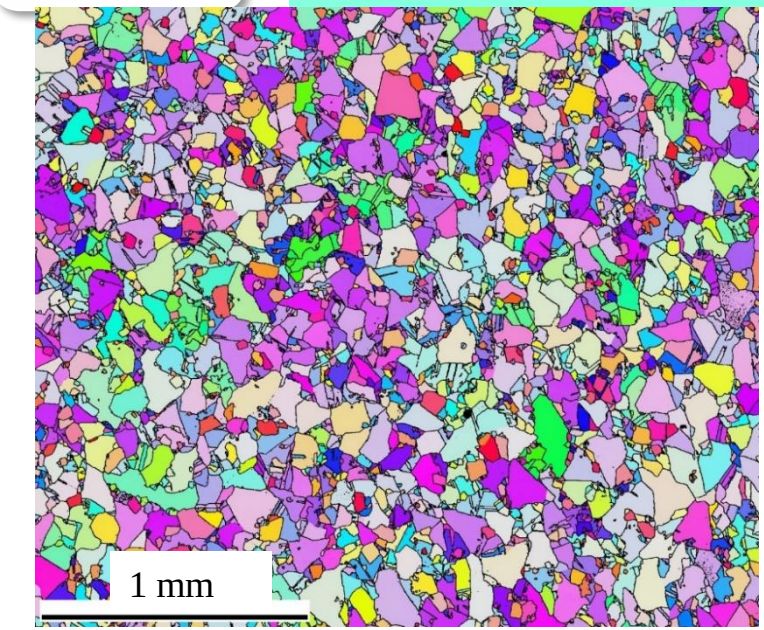

Color coded maps for Xe-irradiated CVD diamond discs (crystallographic directions parallel to the growth direction, irradiated side = growth side, black lines represent boundaries >15° misorientation).

Sample N1, 10^{11} cm^{-2}, 6400 grains (center region)

Sample N4 3.8×10^{13} cm^{-2}, 5900 grains (center region)

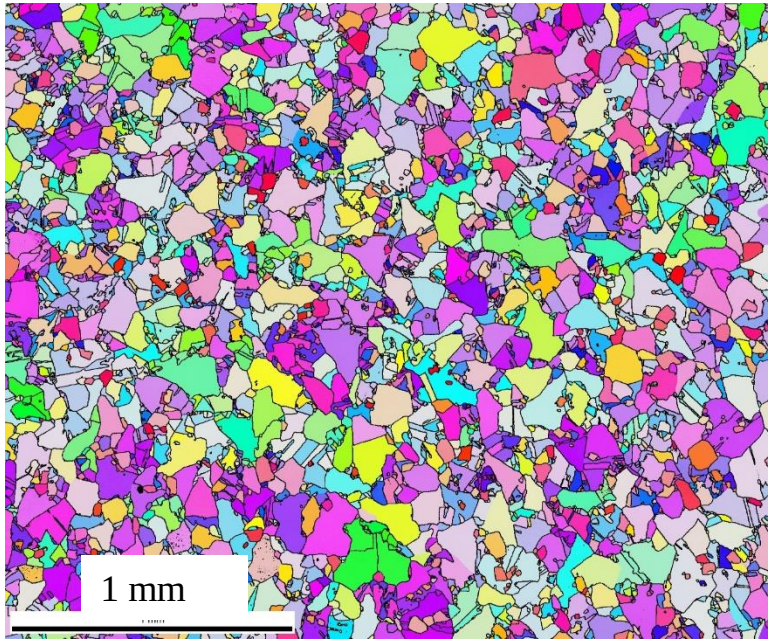

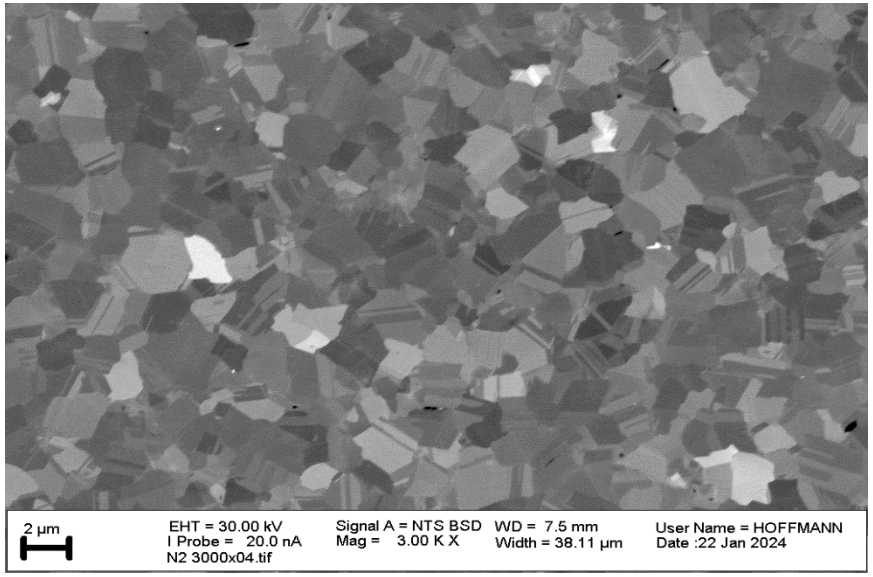

Samples **N2** and **N3** were Xe-irradiated from nucleation site (NS), the grain size was too small to get an EBSD evaluation. Therefore, an electronic backscatter image was measured

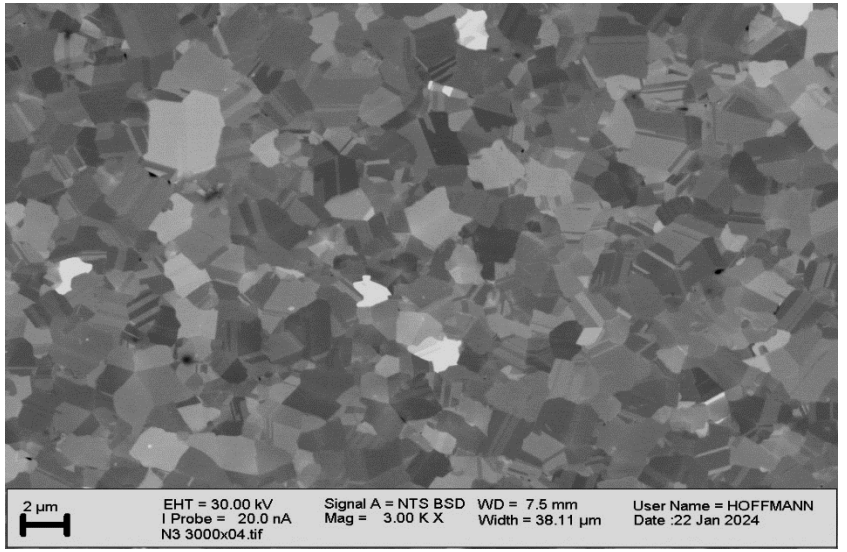

Electron backscatter diffraction (*EBSD*) – grain orientation in polycrystalline diamond

ID	irradiated side	Xe ion fluence /cm^{-2}	average grain size (>15°)by number /µm	average grain size (>15°) by area /µm	fraction all (Σ3) CSL boundary* %
N1	growth side	10E11	22.2	83.5	60 (45)
N2	nucleation side	10E12	x	x	x
N3	nucleation side	10E13	x	x	x
N4	growth side	3.8x10E13	23.7	85.2	60 (43)

Comparison of pristine/irradiated samples shows – there is ***no influence on the surface microstructure*** caused by irradiation with the Xe ions, independent on the ion fluence.
There is no influence of the crystal orientation by irradiation. The defects introduces by irradiation are on a much smaller scale and can not be detected with EBSD technique.

ABOUT PLANNED **Neutron spectroscopy of diamond samples at ILL Grenoble and phonon spectra aqnalysis.**

We planned to use a beamline **IN8 with** a high-flux three-axis thermal neutron spectrometer designed to measure inelastic neutron scattering on single crystals in a wide energy and momentum transfer range.

Problems –– Long-term shutdown due to renovation.

REPORT on test

The diamond single crystalline sample came from KIT (PO#: 20762103) and had dimensions 8×8 mm^2 with a thickness of 45 to 47 mm, leading to a total mass of about 10 mg.

Conclusion on May 2024: **The provided single crystal diamond sample was *to small for measurements***

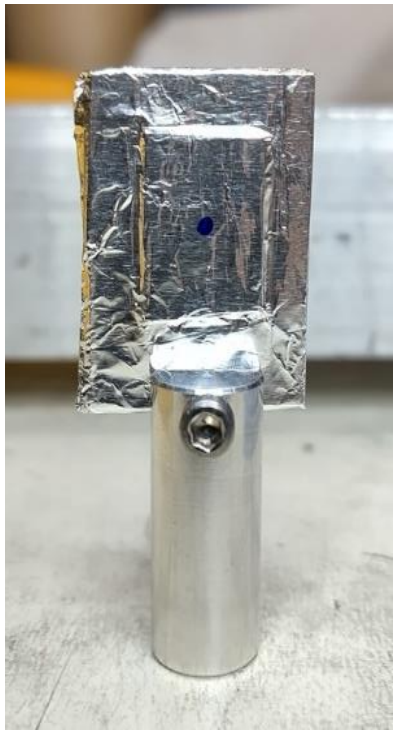

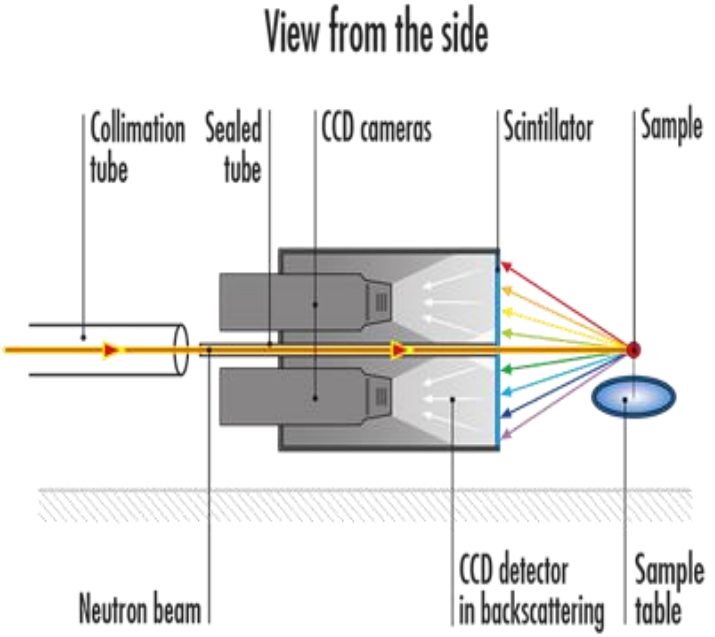

The second, a boron-doped **polycrystalline** diamond sample was used for testing the Laue picture (no Bragg scattering).

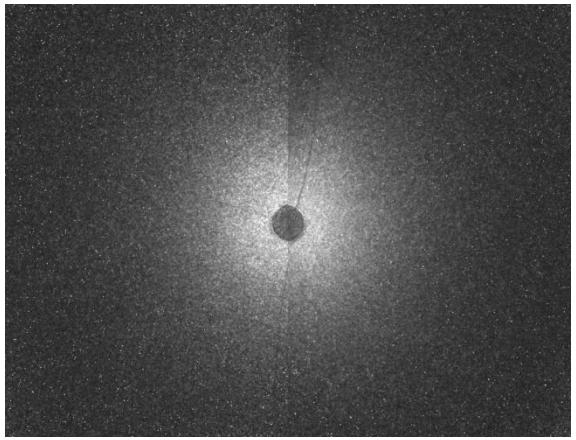

Figure: *Left* – Sample holder used for the Laue measurements. The sample position is indicated by the blue spot.
Right – Schematic view of the Laue instrument OrientExpress @ ILL. Neutron beam is collimated before it transverse the central axis of the camera. After backscattering on the sample, the neutrons are registered by the scintillator/CCD cameras

In near future, Prof. Theo Scherer plans to repeated the measurements at IN8, ILL (Grenoble) with the diamond samples of suitable size/volume (from Japan).

INSTITUTE OF SOLID STATE PHYSICS
UNIVERSITY OF LATVIA

LATVIA

***Computation simulations of** the atomic, electronic, vibrational properties as well as the properties of basic **lattice** defects in **diamond and related materials** (ISSP-UL)*

Theoretical activities included **the first principles calculations** of the atomic, electronic, vibrational properties and dielectric properties of basic defects in ***diamond and AlN***. The state of the art first principles methods using the CRYSTAL17 computer code within the linear combination of atomic orbitals (LCAO) approximation and VASP plane wave code have been used.

For defects in diamond – the **supercells** containing 64 C atoms each and periodically repeated defects; a few basis sets for C, unrestricted DFT with B1WC as well as B3LYP advanced hybrid DFT with exchange-correlation functionals.

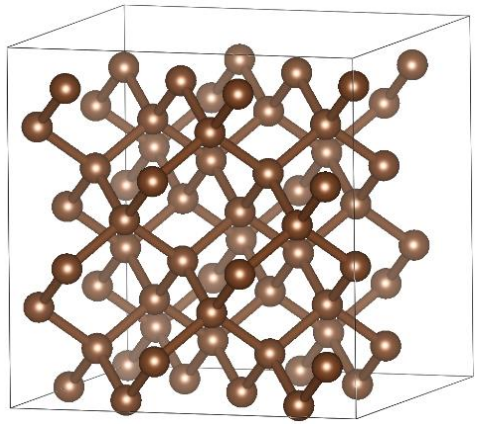

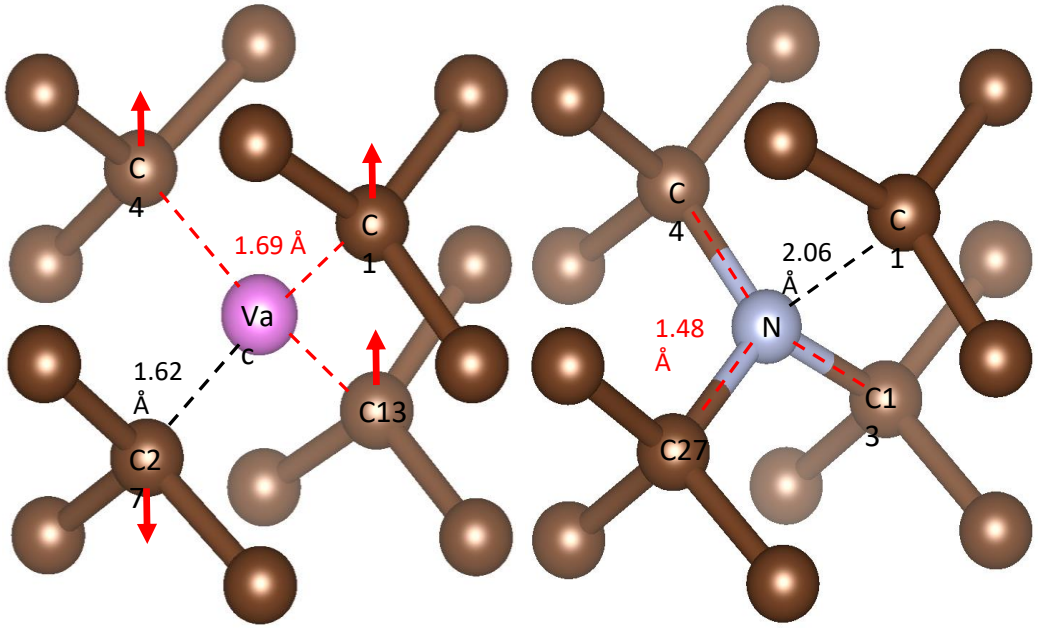

Results of our computational simulation of **a neutral vacancy** (Va, left) and a **nitrogen substitutional atom** (N_s defect, right) in diamond.

INSTITUTE OF SOLID STATE PHYSICS
UNIVERSITY OF LATVIA
LATVIA

(ISSP-UL)

The calculations of harmonic phonon frequencies at the Γ point, IR and Raman spectra, dielectric functions (loss tangent) have been performed for *defective diamond*.

DOS, with a **neutral vacancy**, spin = 0

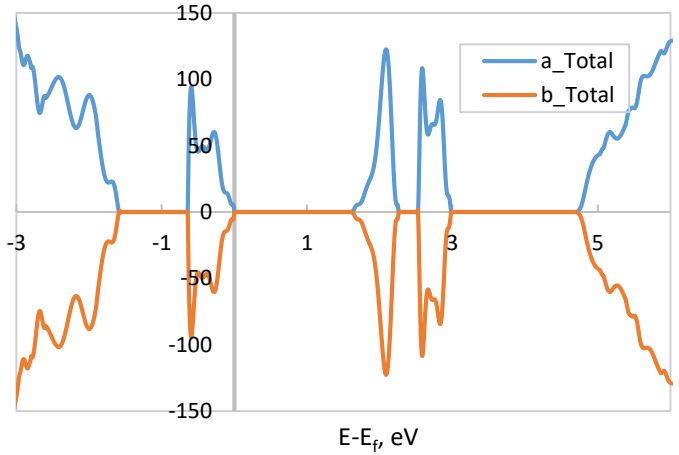

For pristine diamond, E_g = 5.7 eV.

Diamond with vacancy
Raman spectra

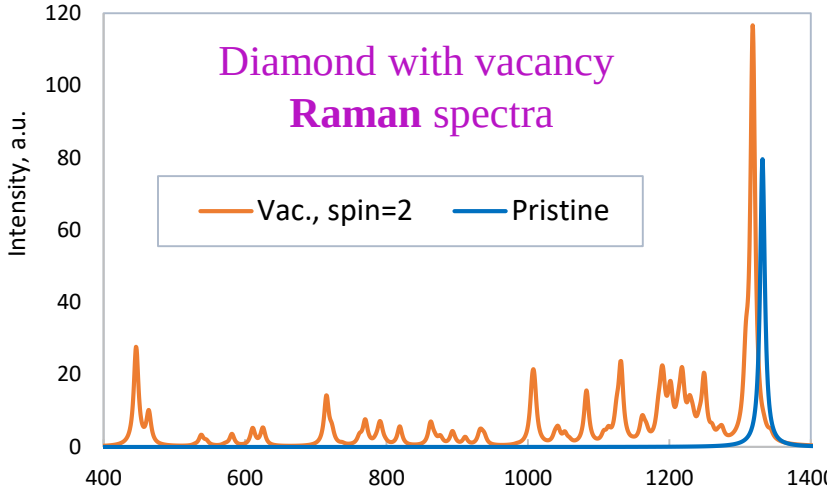

Diamond with N$_s$ defect
Raman spectra

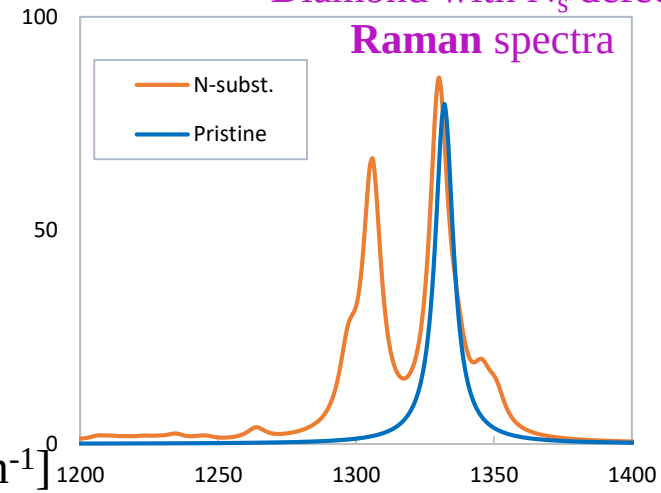

Calculated **Raman** peak for pristine diamond is at 1332 cm^{-1} (coincides with the experimental value). Calculated **loss tangent** for defective diamond in range 140-206 GHz used in monitoring is about 2×10^{-7}.

DOS, diamond with N$_s$ defect

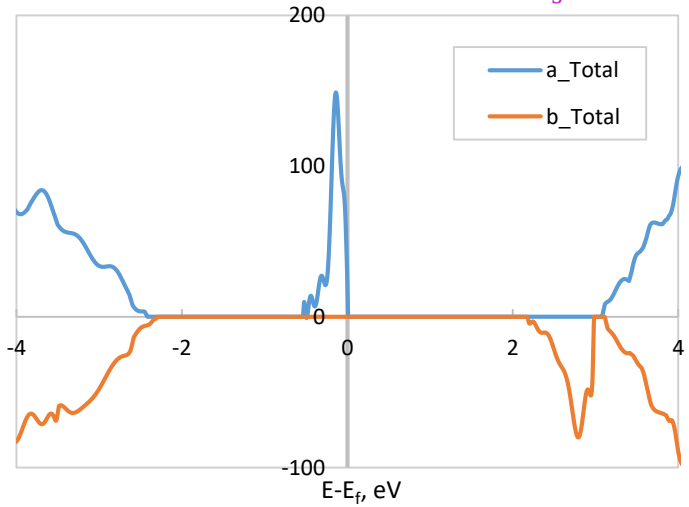

Loss tangent with vacancy, spin=4

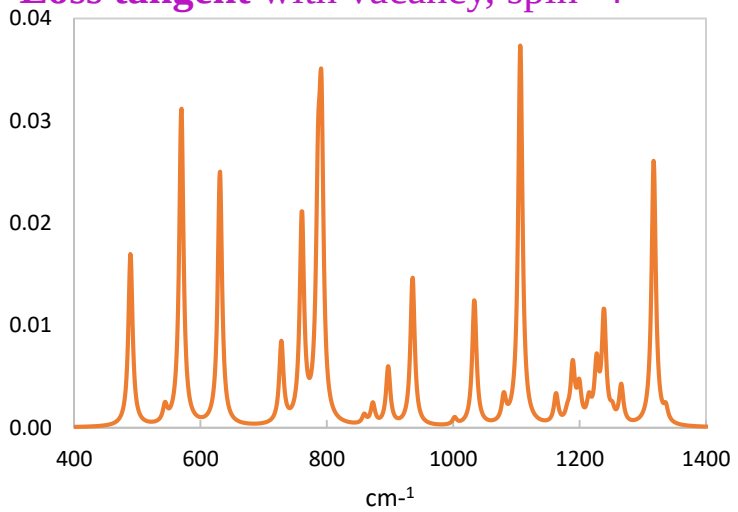

Loss tangent with N$_s$ defect

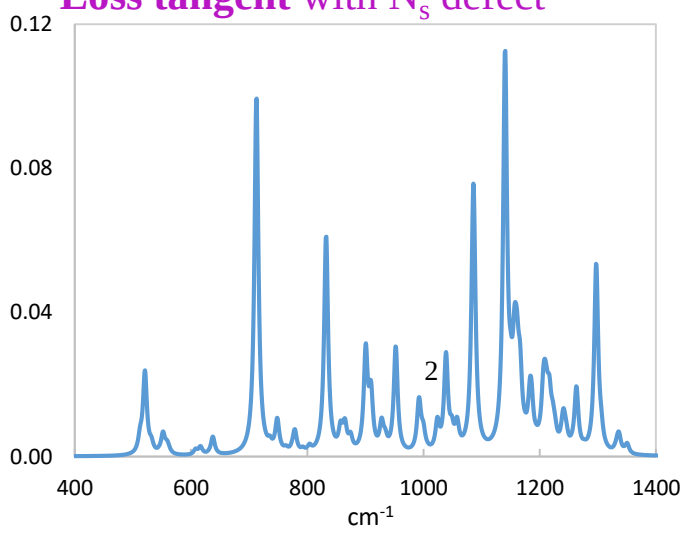

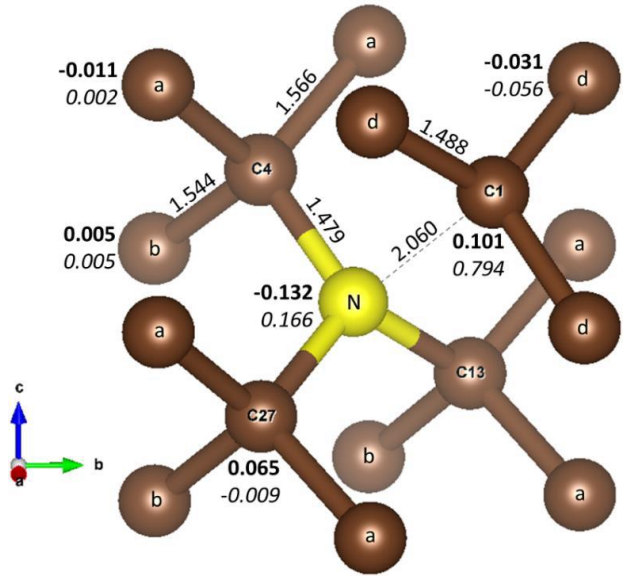

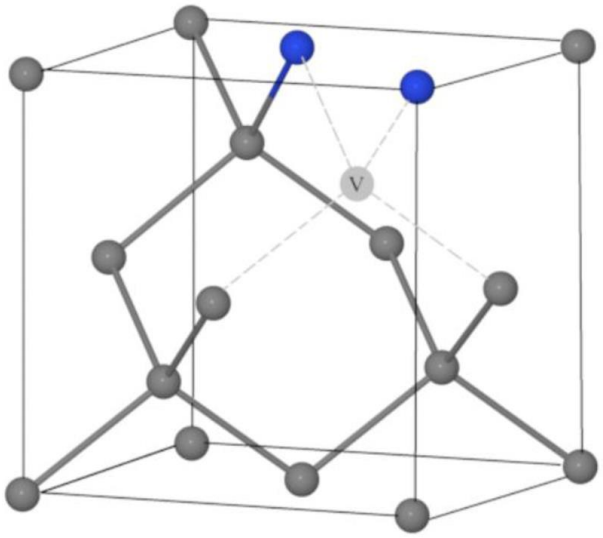

N_2V

The main conclusion on diamond – both defects (V_a, N_s) produce ***negligible (10^{-7}) loss tangent*** in the operational range 140-206 GHz, needed in fusion reactors for plasma heating and stabilization via diamond windows. Other defects such as B or larger pores/surfaces should be checked.

Results of the first principles calculations of the IR, Raman and loss tangent spectra of a **nitrogen substitutional atom** (N_s defect or C center) and in **vacancies** in diamond (Ib diamond) were published in

[9] ***Diamond and Related Materials*** 130 (2022) 109399, *ID35232*
[11] ***Opt. Mater***., 150 (2024) 115222, *ID35232*

The energies and charge and spin distribution of several defects (mono-substitute N in different charge state'; N_s-H and N_2V defects in diamond have been calculated as well:

[6] ***Materials*** **16** (2023) 1979 *ID34871*
[7] ***J. Chem. Phys***. **160** (2024) 034705 *ID36689*
[11] ***Phys. Chem. Chem. Phys***. 2024 DOI: 10.1039/D4CP02309A *ID35808*

INSTITUTE OF SOLID STATE PHYSICS
UNIVERSITY OF LATVIA
LATVIA

First principles calculations of the atomic/electronic structure and the lattice vibrational spectra as well basic radiation defects for **AlN** and have been performed. [12] *Condens. Matter (MDPI) submitted ID36688*

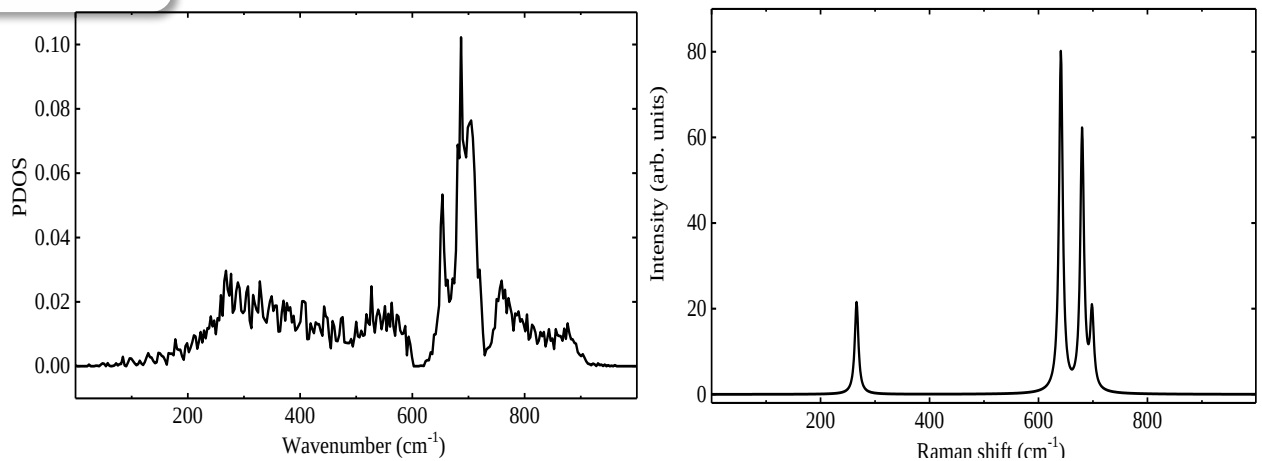

Calculated phonon (*left*) and Raman (*right*) spectra of a perfect AlN.

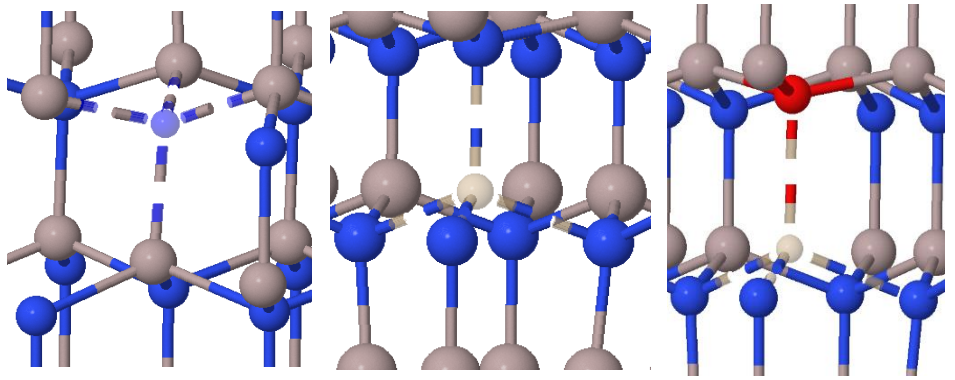

Basic defects modelled in AlN (Al – brown, N – blue): N vacancy (*left*), Al vacancy (*middle*) and V_{Al}-O complex (*right*, O – red).

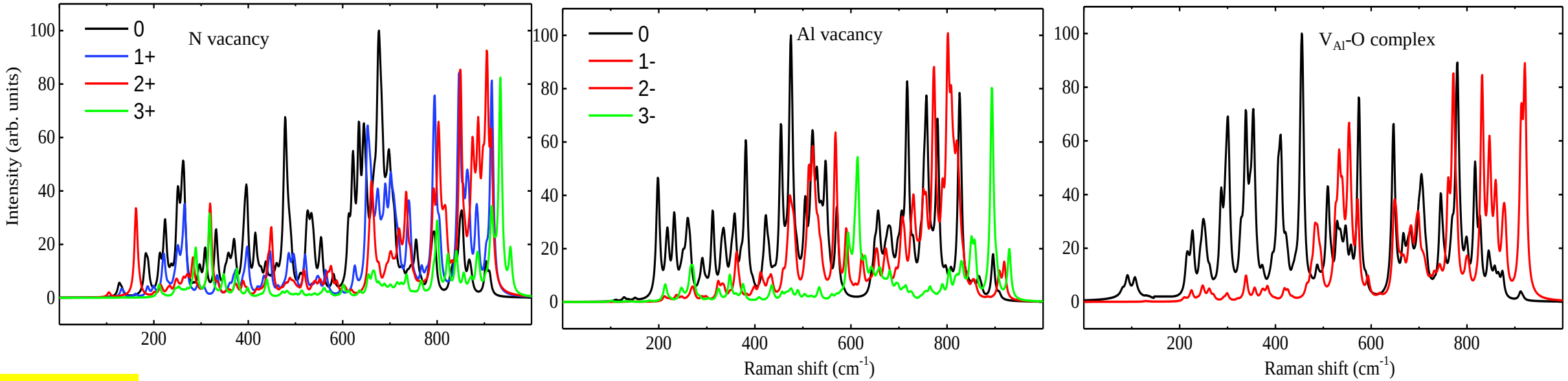

(ISSP-UL)

The Raman spectra calculated for **N and Al vacancies** in different charge states as well as for **V_{Al}-O complex**.

INSTITUTE OF SOLID STATE PHYSICS
UNIVERSITY OF LATVIA

LATVIA

Annealing kinetics of radiation defects measured via the EPR method … in alumina

Alumina transparent ceramic disks, irradiated by fast neutrons ($E > 0.1$ MeV, fluences of 10^{21}, 10^{22} and $10^{23} n/m^2$) at Joint Research Center (Petten, Netherlands).

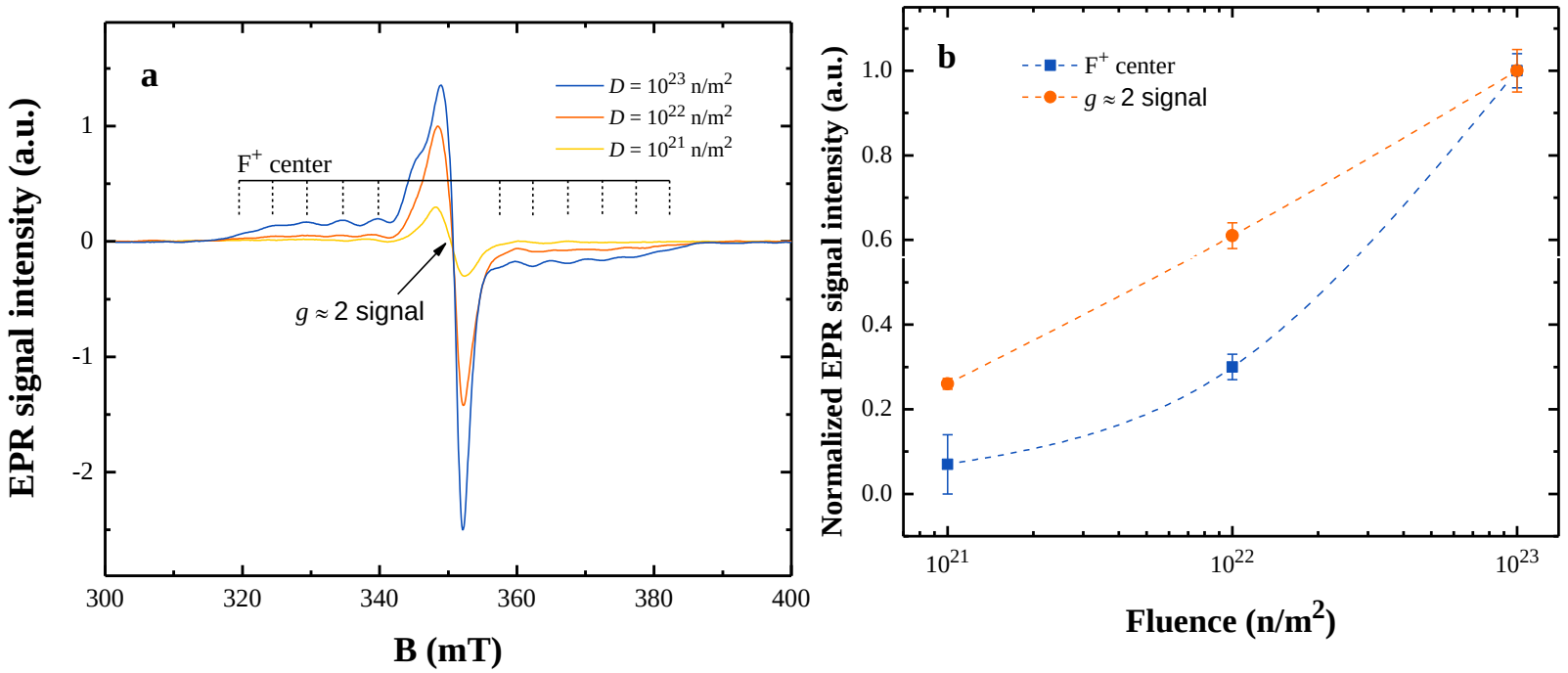

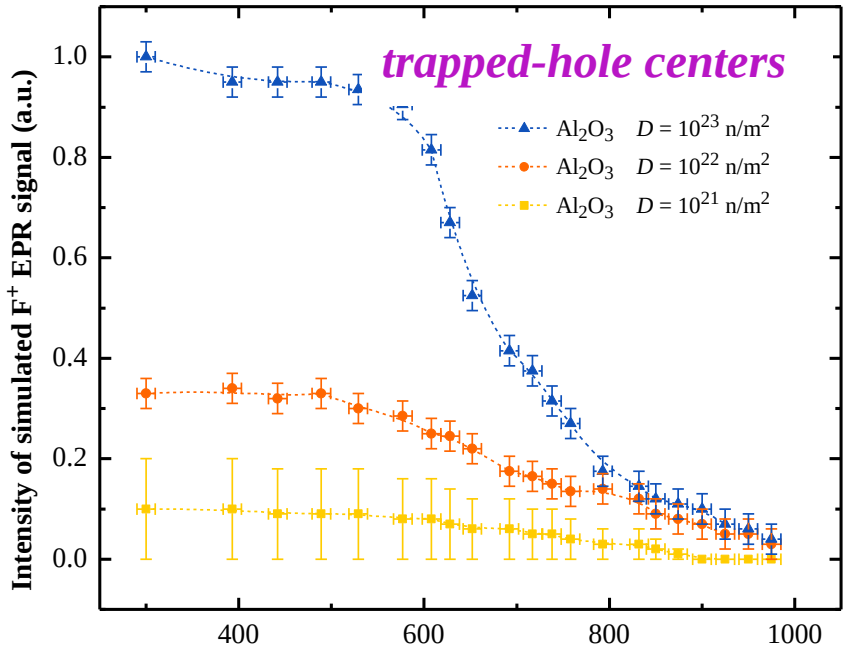

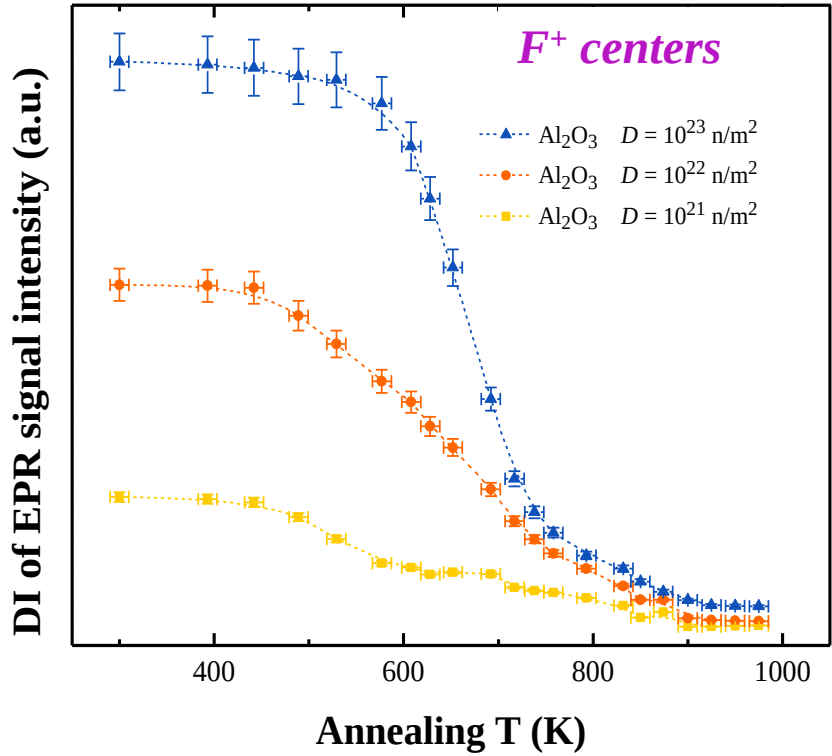

F$^+$ center signal is optimized at investigated at field modulation amplitude 1.5 mT and microwave power *P* = 0.06325 mW.
For "g~ 2" defects (**trapped-hole centers**): 0.3 mT and *P* = 0.6325.

[2] *Opt. Mater.* **135** (2023) 113250, *ID33491*

INSTITUTE OF SOLID STATE PHYSICS
UNIVERSITY OF LATVIA

LATVIA

Experimentally measured annealing kinetics of EPR-active radiation defects and their theoretical modelling … in neutron-irradiated silica

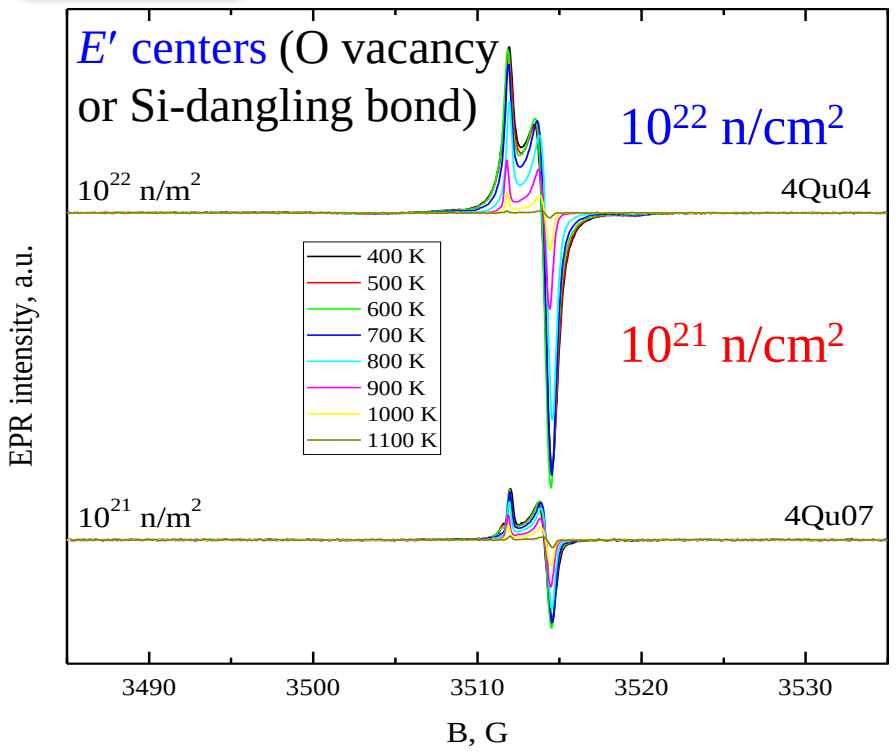

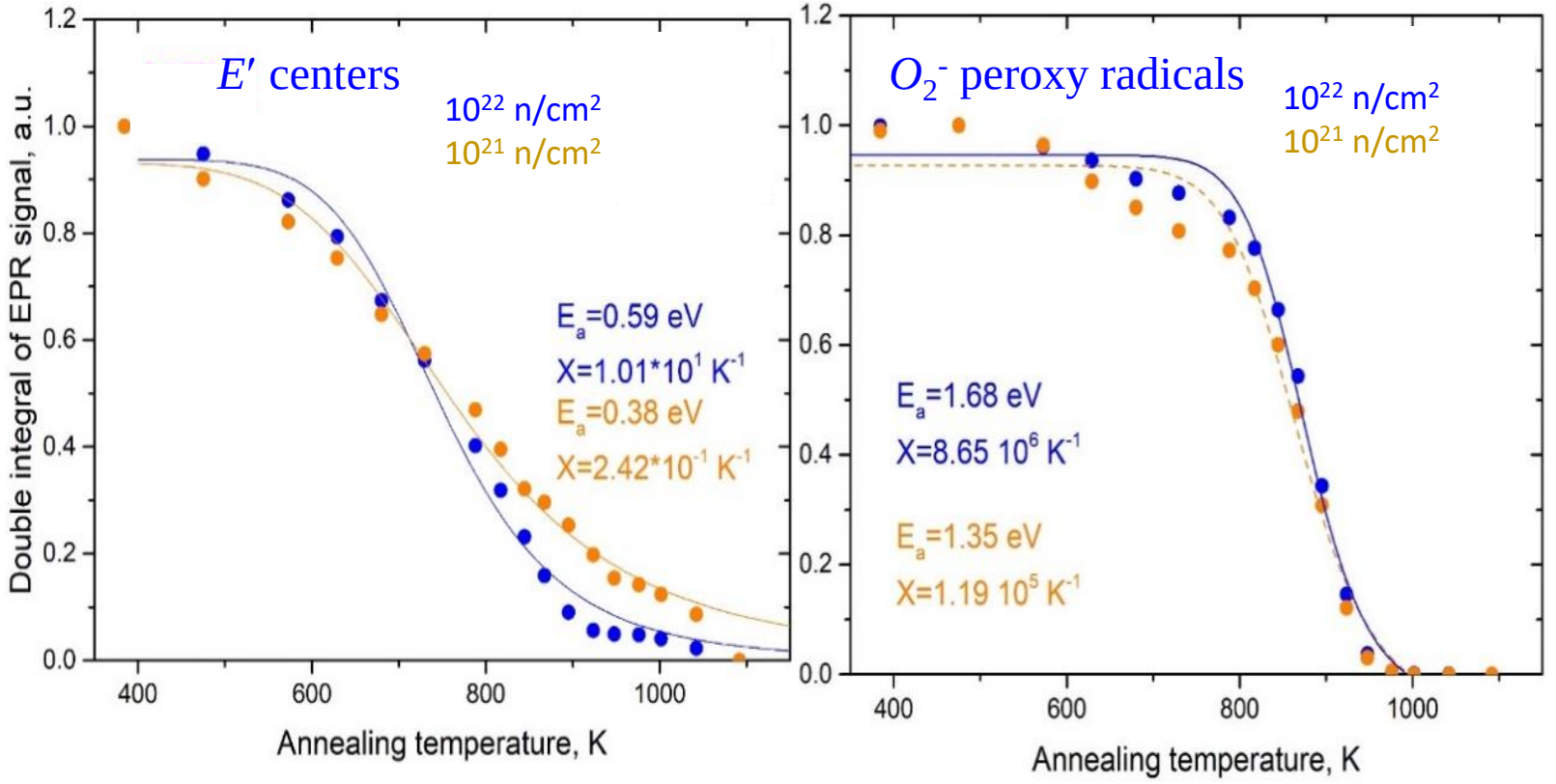

Detection conditions for *E′* center:
P =1 μW; 0.1 G modulation amplitude; **B** at 3512 ± 30 G.

Detection conditions for O_2^- peroxy radicals:
P = 200 mW

[13] ***Opt. Mater.*** *sumbitted, ID36710*

Normalized annealing kinetics for the *E′* centers (*left*) and O_2^- radicals (*right*) in neutron-irradiated silica. Symbols – experimental points via the EPR, lines – theoretical analysis in terms of diffusion-controlled recombination reactions.
Conclusions: for both defects ther migration energy depends on dose! Quantum chemical calculations are needed for final interpratation of recombination mechanism. *Suggestion*: mobile non-bonding oxygen atoms recombine with *E′*, while O atoms diffusion causes the decay of peroxy radicals.

INSTITUTE OF SOLID STATE PHYSICS
UNIVERSITY OF LATVIA
LATVIA

Experimentally measured annealing kinetics of radiation defetcs and their theoretical modelling … in silica

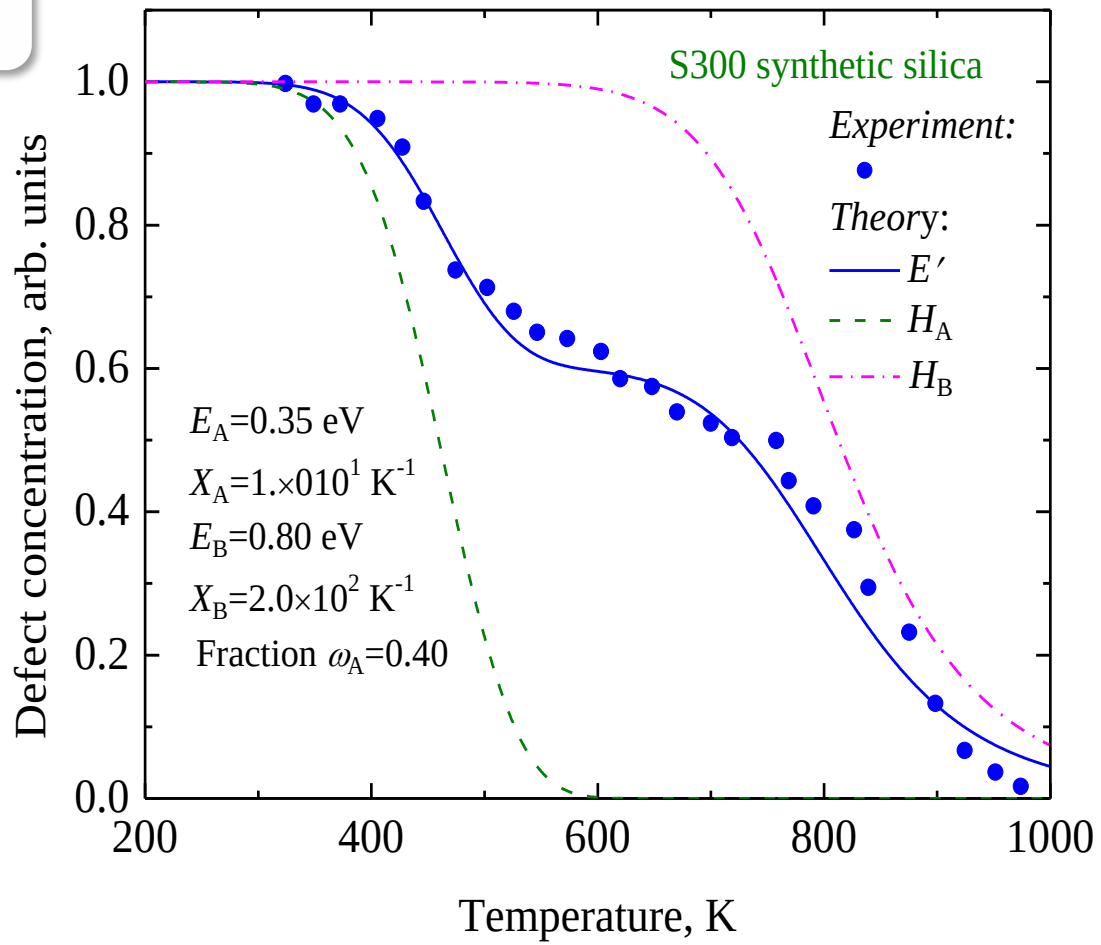

Figure. The experimental annealing kinetics of the *E*' centers (symbols) in a dry synthetic S300 silica with 1 ppm of OH (from Ref. [12]). Lines – theory for the *E*' (solid) and complementary oxygen interstitials (dashed).

Theoretical analysis of the defect annealing in silica samples with different OH content irradiated by neutrons or gamma-rays (from literature data).

The kinetics is modelled in terms of *diffusion-controlled bimolecular reactions and* assuming **two types of oxygen interstitials,** which recombine with immobile *E′* centers (an oxygen vacancy). The estimated migration energies E_a of interstitials are 0.35 and 0.80 eV, respectively (dotted lines).

Mobile interstitials (labelled as H_A and H_B) are tentatively associated with the non-bridging oxygen hole centers and the O_2^- peroxy radicals.

[5] ***J. Nucl. Mater***. 579 (2023) 154381. *ID34869*

University of Tartu
ESTONIA

Annealing kinetics of radiation defects measured via optical absorption (UT)

5-mm-diameter (0.4 mm thickness, *Diamond Materials, Freiburg*) novel disks of CVD diamond have been characterized via ***optical absorption,*** *EBSD, CL, FTIR and Raman* methods before and after irradiation by 231-MeV ^{132}Xe ions at RT (Astana Kazakhstan) with 4 different fluences. According to SRIM, ion range R= 18.7 μm.

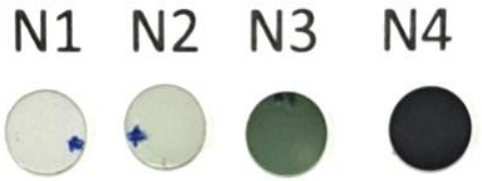

10^{11} 10^{12} 10^{13} 3.8×10^{13} Xe/cm^2

Absorption spectra for pristine and irradiated CVD diamond disks. RT, JASCO-V660 spectrophotometer.

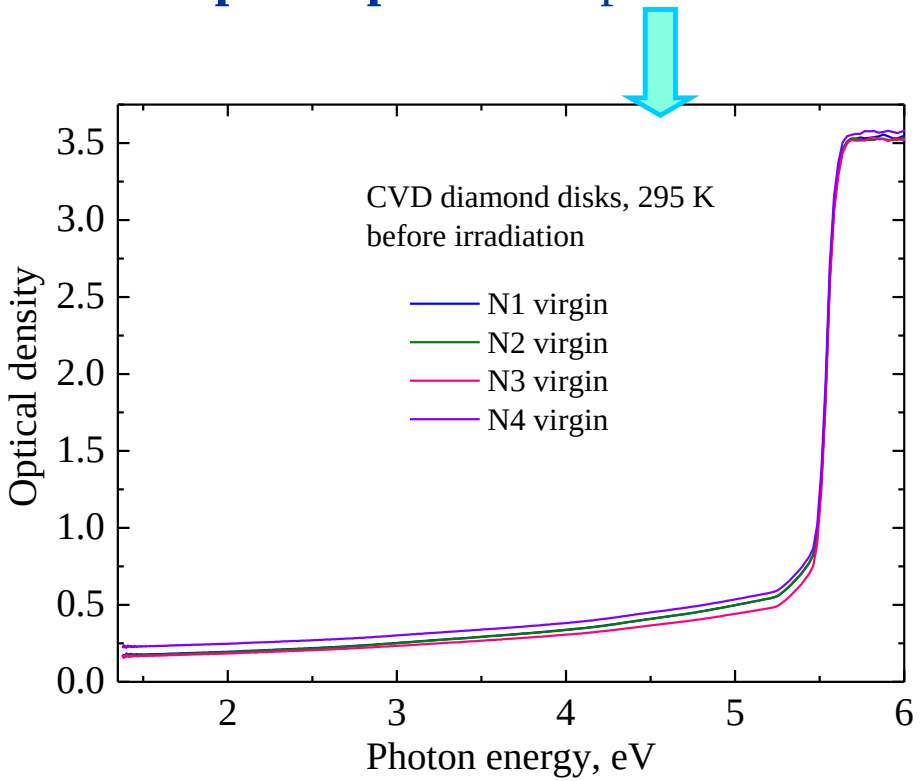

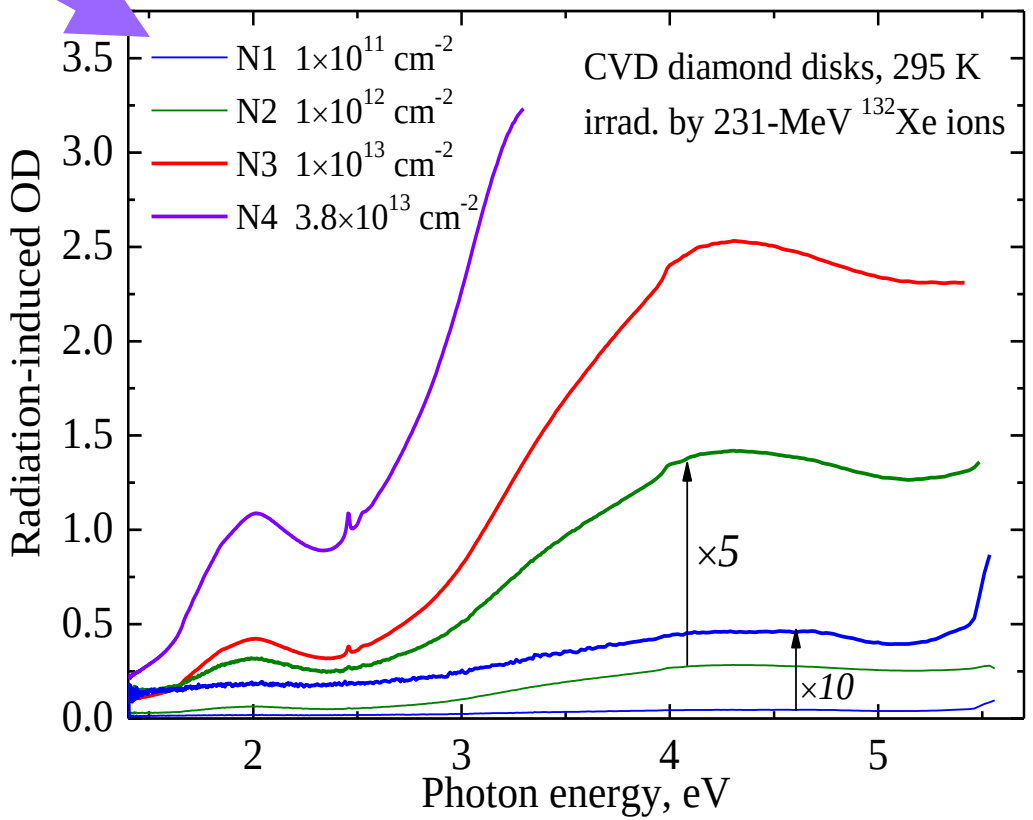

Figure. RIOA spectra of CVD diamond disks (absorption of pristine sample is subtracted) exposed to 231-MeV xenon ions with different fluences. For best visualization low-fluence curves are multiplied by a certain factor.

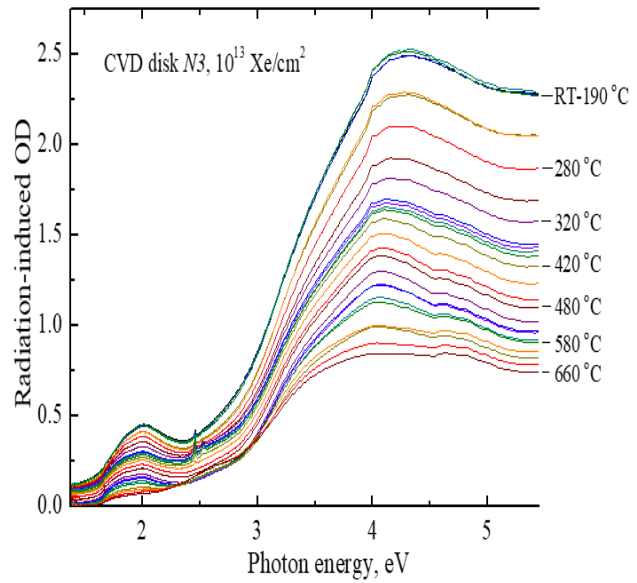

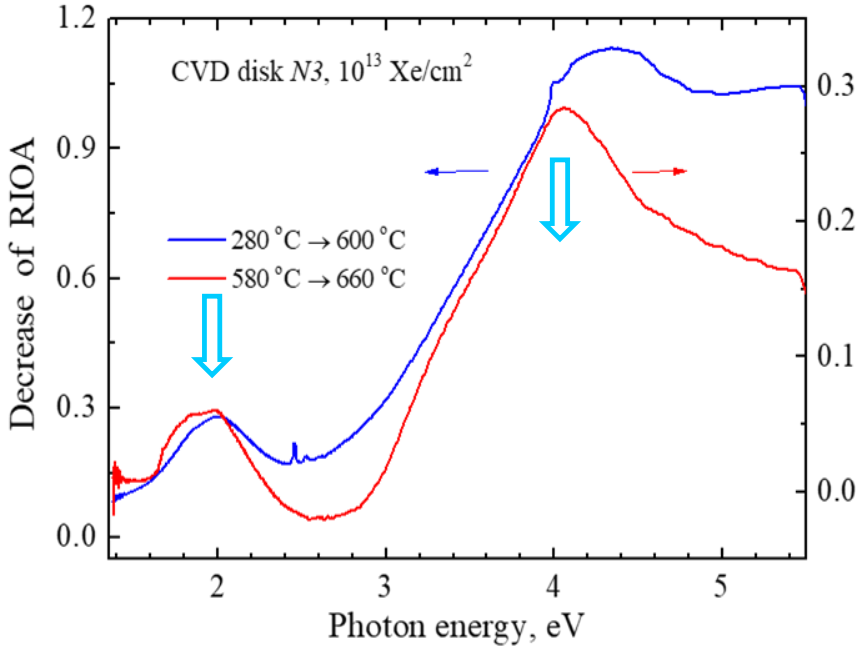

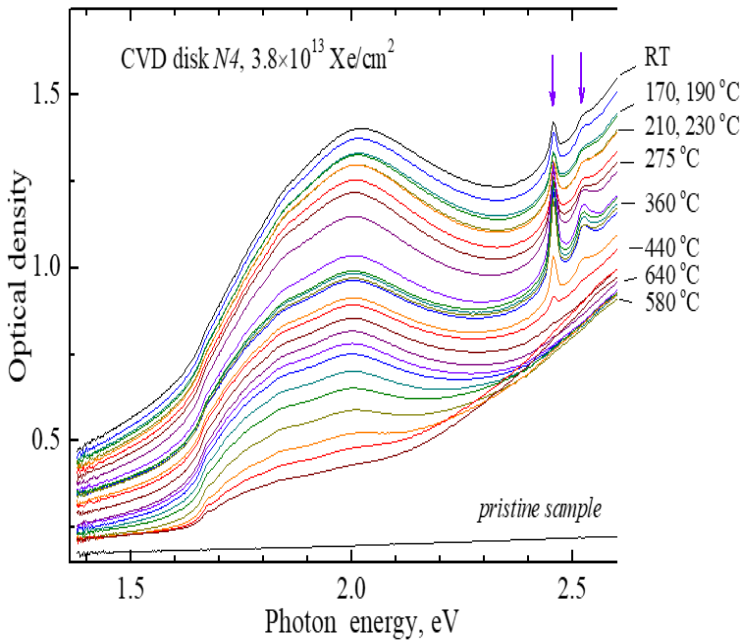

The carbon vacancies (GR1, a neutral vacancy) are mainly responsible for RIOA around 2 eV, while complementary C-interstitial-related defects R11 tentatively absorb at about 4 eV (i.e. a ***carbon interstitial-vacancy Frenkel pair***).

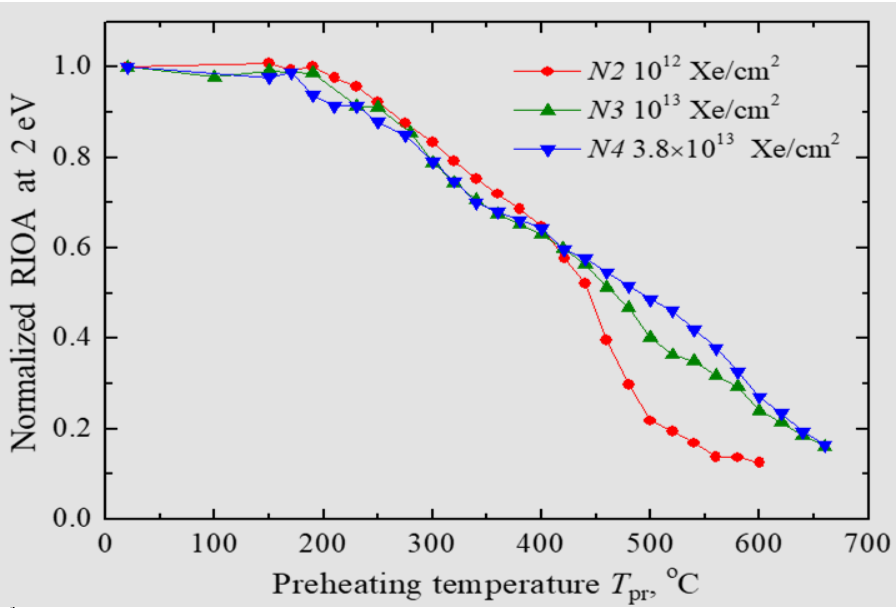

Narrow bands around 2.5 eV are tentatively nitrogen-related complex defects, a number of which was detected in Raman and FTIR spectra of the same pristine and Xe-irradiated CVD diamond samples.

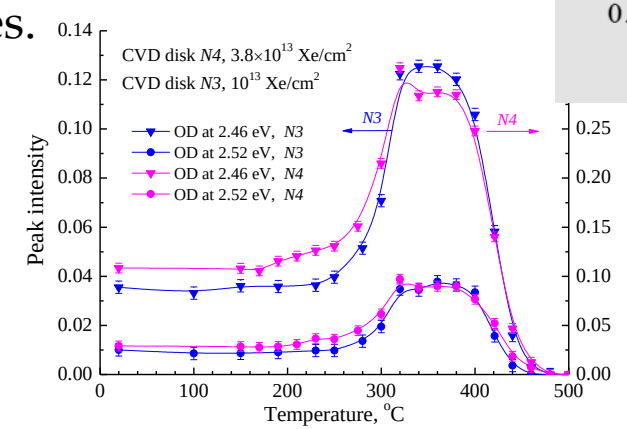

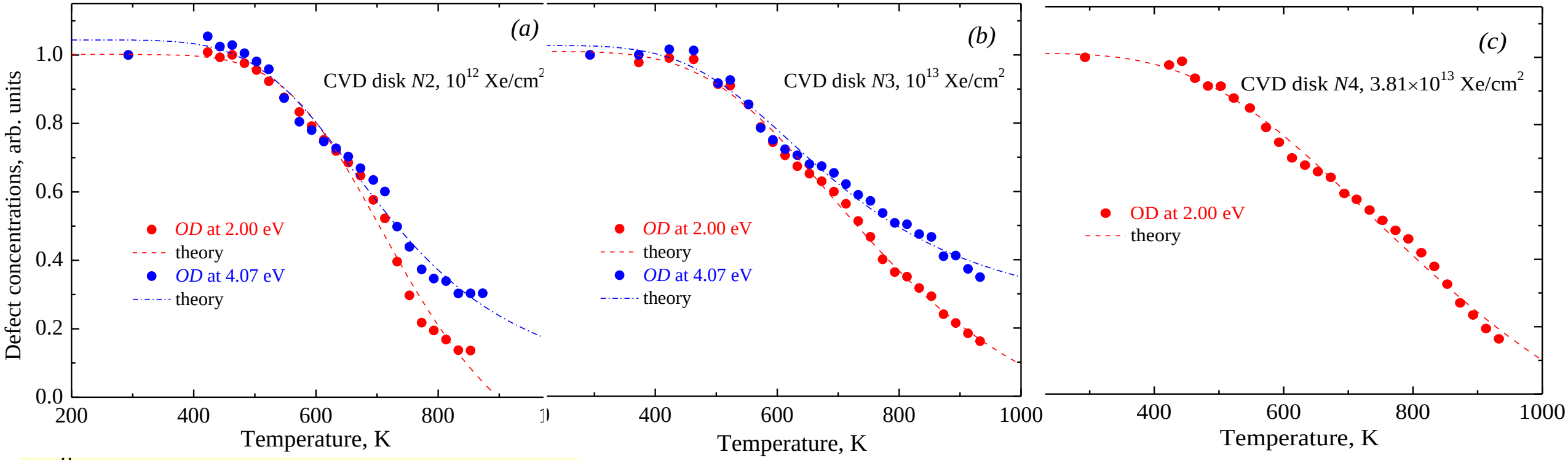

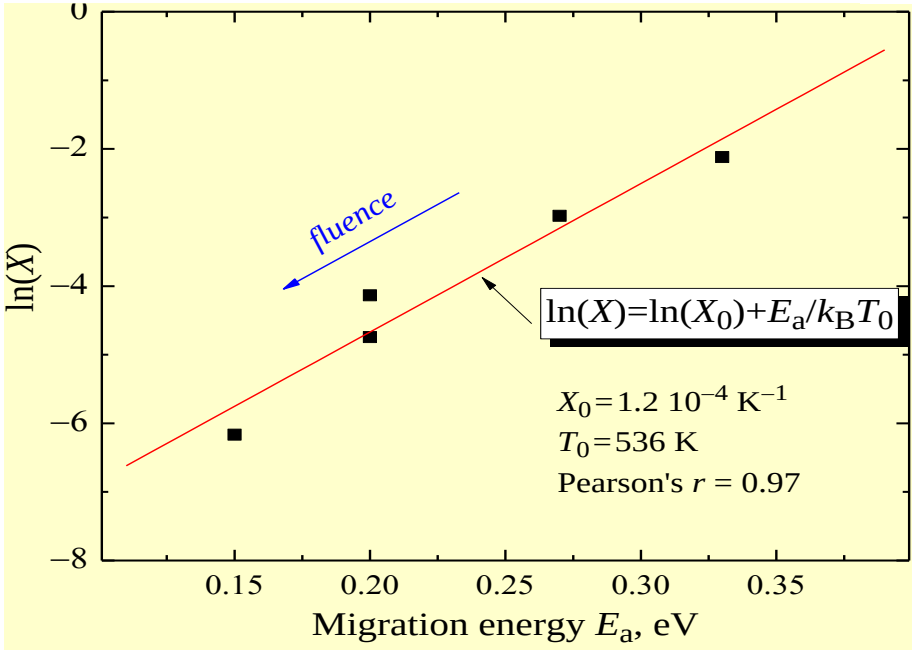

Theoretical analysis of the experimental kinetics of interstitial-vacancy carbon Frenkel defects (absorption at 4.1 eV and 2.0 eV, respectively) in CVD diamond disks shows the migration energy of the interstitial ions as quite low, of the order of 0.2-0.4 eV, that could be related to a strong structural distortion upon heavy swift ion irradiation. The diffusion prefactors X show a very good correlation with the migration E_a, which is known as the Meyer-Neldel rule in chemical kinetics.

[10] ***Crystals*** 14, (2024) 546 *ID38109*

Publications related to the project

[1] L.L. Rusevich, E.A. Kotomin, A.I. Popov, G. Aiello, T.A. Scherer, A. Lushchik. The vibrational and dielectric properties of diamond with N impurities: First principles study. *Diamond Relat. Mater.* **130** (2022) 109399. doi:10.1016/j.diamond.2022.109399 *ID33490*

[2] A. Antuzevics, E. Elsts, M. Kemere, A. Lushchik, A. Moskina, T.A. Scherer, A.I. Popov, Thermal annealing of neutron irradiation generated paramagnetic defects in transparent Al_2O_3 ceramics. *Opt. Mater.* **135** (2023) 113250. doi:10.1016/j.optmat.2022.113250 *ID33491*

[3] V. Seeman, A.I. Popov, E. Shablonin, E. Vasil'chenko, A. Lushchik, EPR-active dimer centers with S = 1 in α-Al_2O_3 single crystals irradiated by fast neutrons, *J. Nucl. Mater.*, **569** (2022) 153933. doi:10.1016/j.jnucmat.2022.153933 *ID33492*

[4] N. Mironova-Ulmane, M.G. Brik, J. Grube, et al., EPR, optical and thermometric studies of Cr^{3+} ions in the α-Al_2O_3 synthetic single crystal, *Opt. Mater.* **132** (2022) 112859. doi:10.1016/j.optmat.2022.112859 *ID33493*

[5] V. Kuzovkov, E. Kotomin, R. Vila, Theoretical analysis of thermal annealing kinetics of radiation defects in silica, *J. Nucl. Mater*. **579** (2023) 154381. doi:10.1016/j.jnucmat.2023.154381 *ID34869*

[6] A. Platonenko, W.C. Mackrodt, R. Dovesi, The Electronic structures and energies of the lowest excited states of the N_s^0, N_s^+, N_s^- and N_s-H defects in diamond, *Materials* **16** (2023) 1979. doi:10.3390/ma16051979 *ID34871*

[7] W.C. Mackrodt, A. Platonenko, F. Pascale, R. Dovesi, The energies and charge and spin distributions in the low-lying levels of singlet and triplet N_2V defects in diamond from direct variational calculations of the excited state, *J. Chem. Phys*. **160** (2024) 034705. doi:10.1063/5.0178893 *ID36689*

[8] E. Feldbach, A. Krasnikov, A.I. Popov, V. Seeman, E. Shablonin, A. Lushchik, Cathodoluminescence as a tool for monitoring radiation damage recovery in corundum, *J. Lumin.* (2024) 120490. doi:10.1016/j.jlumin.2024.120490 *ID36711*

[9] L.L. Rusevich, A. Lushchik, T.A. Scherer, G. Aiello, A.I. Popov, E.A. Kotomin, The electronic, vibrational and dielectric properties of diamond crystals with neutral vacancies: First principles study. *Opt. Mater.*, 150 (2024) 115222 *ID35232*

[10] E.A. Kotomin, V.N. Kuzovkov, A. Lushchik, A.I. Popov, E. Shablonin, T. Scherer, E. Vasil'chenko, The annealing kinetics of defects in CVD diamond irradiated by Xe ions, *Crystals* 14, (2024) 546. https://doi.org/10.3390/cryst14060546 *ID38109*

[11] A. Platonenko, F.S. Gentile, K. E. El-Kelany, R. Dovesi, The role of the exact Hartree-Fock exchange in the in-vestigation of defects in crystalline systems, *Phys. Chem. Chem. Phys.*, 2024, DOI: 10.1039/D4CP02309A *ID35808*

[12] A. Platonenko, E.A. Kotomin, A. Popov, Hybrid DFT calculations on vibrational properties of vacancy defects in hexagonal AlN crystals, *Condensed Matter (MDPI), submitted ID36688*

[13] A. Antuzevics, A.I. Popov, T.A. Scherer, V.N. Kuzovkov, E.A. Kotomin, A. Lushchik, Thermal annealing of radiation defects in neutron irradiated silica, *Opt. Mater.*, submitted *ID36710*

Aleksandrs Platoņenko, First principles modelling and characterization of radiation point defects in α-Al_2O_3 and $MgAl_2O_4$ crystals, ***PhD (in Physics)*** *Thesis*, Supv. Deniss Grjaznovs, University of Latvia (2023). https://dspace.lu.lv/dspace/handle/7/63041

Alise Podelinska, Vibrational spectroscopy of radiation resistive ceramics for fusion applications, ***Master Thesis***, Supv. Anatolijs Popovs, University of Latvia (June 2023). https://dspace.lu.lv/dspace/handle/7/64355

Main conclusions and suggestions

CVD diamond shows no structural defects in the order of grain size (size and distribution); there is no influence of the crystal orientation by irradiation. Single crystalline diamond shows no structural (large size crystal defects via ***EBSD*** measurements as well.

The single 1332-cm^{-1} ***Raman*** mode in CVD diamond broadens, shifts to lower frequencies, and transforms to asymmetric with irradiation fluence – ***a local structural disorder*** induced in diamond samples by Xe-irradiation.

Based on ***FTIR*** measurements, Xe-irradiation leads to the the appearance of N defect bands at 1700-500 cm^{-1} (not detectable in a pristine CVD diamond) tentatively due to radiation-induced modification in the state of N defects On the other hand, the analysis of the characteristic C–C band at 2600-1600 cm^{-1} shows no significant alteration with Xe-irradiation.

The degradation of CVD disks starts above 650 °C and prevents a total annealing of radiation damage (recovery from damage) measured via ***radiation-induced optical absorption***.

Advanced theoretical analysis of the defect annealing under different fluencies ***allows to predict*** the kinetics of defect accumulation under different external conditions.

Based on ***theoretical calculations***, diamond lattice defects such as V_a, and N_s produce negligible (10^{-7}) loss tangent in the operational range 140-206 GHz, needed in fusion reactors for plasma heating and stabilization via diamond windows.

Impact for fusion applications: for a certain nuclear environment in fusion reactor parts (heating and diagnostic systems, with lower radiation influence!) →

Diamond is an excellent appropriate material for such applications.

In case of SC diamond, there are much lower dielectric losses. In Japan companies, the so-called mosaic SCD wafers (original from AIST in Osaka) are quickly developing. The price of Lab Grown Diamond windows (LGD) drops in time significantly! This could be the future of FM in Fusion research in the development phases in EUROfusion programs.

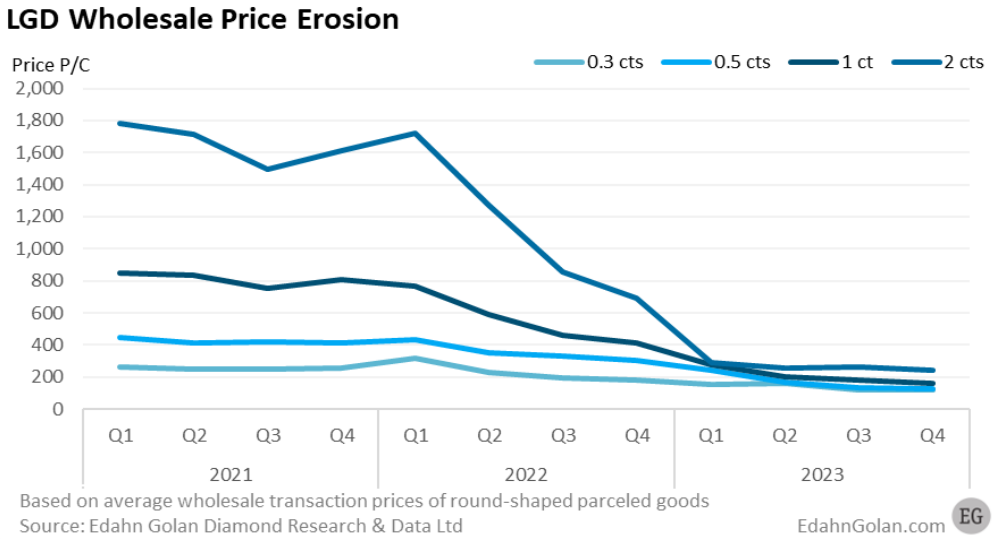

<u>Recommendations for WP implementations in future in EUROfusion:</u>

- Incorporate mosaic SCD samples and wafers into EUREOfusion FM-ENR-programs to improve dielectric losses for heating and current drive and diagnostic windows as well.
- Check by spectroscopic measurements (RAMAN, CL, PL, ESR, etc. …) the optical properties.
- Check especially the content of nitrogen and gaphite like sp2 carbon, which will implemented in SCDs due to the mosaic SCD production process.
- All these investigations could provide for a DEMO reactor a quasi-new diamond quality with acceptable manufacturing prices!